Supramolecular Chemistry
Publication details, including instructions for authors and subscription information:
http://www.informaworld.com/smpp/title~content=t713649759

Complexation of M^3 Lanthanide Cations by Calix[4]arene-CMPO Ligands: A Molecular Dynamics Study in Methanol Solution and at a Water/Chloroform Interface

L. Troxler[a]; M. Baaden[a]; V. Böhmer[b]; G. Wipff[a]
[a] Institut de Chimie, Université Louis Pasteur, Strasbourg, France [b] Johannes Gutenberg Universität, Fachbereich Chemie und Pharmazie, Mainz

To cite this Article Troxler, L. , Baaden, M. , Böhmer, V. and Wipff, G.(2000) 'Complexation of M^3 Lanthanide Cations by Calix[4]arene-CMPO Ligands: A Molecular Dynamics Study in Methanol Solution and at a Water/Chloroform Interface', Supramolecular Chemistry, 12: 1, 27 — 51
To link to this Article: DOI: 10.1080/10610270008029803
URL: http://dx.doi.org/10.1080/10610270008029803

SUPRAMOLECULAR CHEMISTRY, Vol. 12, pp. 27-51
Reprints available directly from the publisher
Photocopying permitted by license only

Complexation of M^{3+} Lanthanide Cations by Calix[4]arene-CMPO Ligands: A Molecular Dynamics Study in Methanol Solution and at a Water / Chloroform Interface

L. TROXLER [a], M. BAADEN [a], V. BÖHMER [b] and G. WIPFF [a*]

[a]*Institut de Chimie, Université Louis Pasteur, UMR CNRS 7551, 4, rue B. Pascal, 67 000 Strasbourg France and* [b]*Johannes Gutenberg Universität, Fachbereich Chemie und Pharmazie, Abteilung Lehramt Chemie, Duesbergweg 10-14, D-55099 Mainz*

We report a molecular dynamics study on the 1:1 M^{3+} lanthanide (La^{3+}, Eu^{3+} and Yb^{3+}) inclusion complexes of an important extractant molecule **L**: a calix[4]arene-tetraalkyl ether substituted at the wide rim by four NH-C(O)-CH_2-P(O)Ph_2 arms. The $M(NO_3)_3$ and MCl_3 complexes of **L** are compared in methanol solution and at a water / chloroform interface. In the different environments the coordination sphere of M^{3+} involves the four phosphoryl oxygens and three to four loosely bound carbonyl oxygens of the CMPO-like arms. Based on free energy simulations, we address the question of ion binding selectivity in pure liquid phases and at the liquid-liquid interface where **L** and the complexes are found to adsorb. According to the simulations, the enhancement of M^{3+} cation extraction in the presence of the calixarene platform, examined by comparing **L** to the $(CMPO)_4$ "ligand" at the interface, is related to the fact that (i) the $(CMPO)_4Eu(NO_3)_3$ complex is more hydrophilic than the $LEu(NO_3)$ one and (ii) the free CMPO ligands spread at the interface, and are therefore less organized for cation capture than **L**.

Keywords: lanthanide, calixarene, recognition, interface, molecular dynamics

INTRODUCTION

The search for extractant molecules which are highly selective for cations like lanthanides M^{3+} or actinides is a problem of both fundamental and technological importance, especially in the context of nuclear waste management[1–4]. Combination of several ligating functions in a suitable geometrical arrangement on an appropriate scaffold often leads to their cooperative action. Thus, calix[4]arenes bearing four NH-C(O)-CH_2-P(O)Ph_2 CMPO-like groups at the wide rim and various alkyl ethers at the narrow rim were found to be tremendously strong extractants of europium, thorium, neptunium, plutonium and americium cations, from acidic aqueous solutions into organic phases[5]. Transport studies through supported liquid-membranes also demonstrated their higher extraction efficiency, compared to CMPO itself[5–7]. Although the exact nature and composition of the extracted complexes is not yet known, it is evident that the preorganization of the CMPO-like arms anchored at the calix[4]arene platform is an important feature of these ligands.

In this paper, we report a series of computer modelling experiments on three lanthanide complexes of a model ligand **L** (see chart 1) in the cone conformation, bearing four CMPO-like

* Author for correspondence.

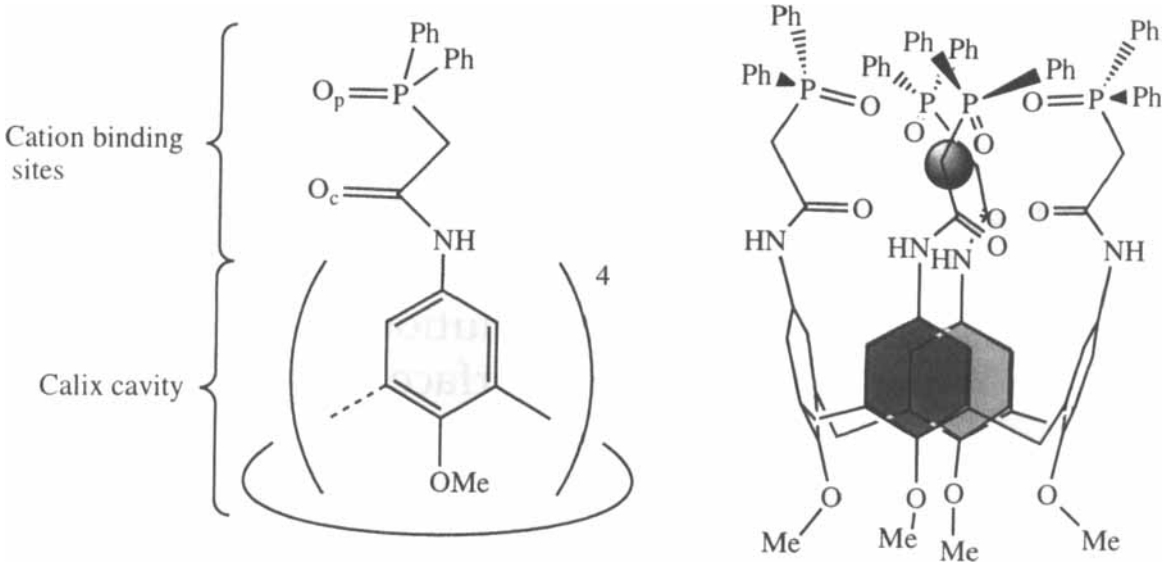

CHART 1 Schematic representation of the calix[4]arene-CMPO ligand **L** (cone conformation) and of a M^{3+} inclusion complex

arms at the wide rim, and four methoxy substituents at the narrow rim. We assume that the complexes are of 1:1 stoichiometry and that the lower rim O-alkyl groups, not directly involved in the cation binding, can be modelled by O-Me groups. As cations, we consider La^{3+}, Eu^{3+} and Yb^{3+}, which represent a "large", "average" and "small" lanthanide cation with their ionic radii being 1.032, 0.947 and 0.868 Å, respectively[8,9]. Our aim is to compare the binding mode of M^{3+}as a function of the cation size, the solvent environment (methanol / liquid-liquid interface), and the counterions (Cl^- / NO_3^-). Do the four CMPO branches bind equally well to M^{3+}? What is the strain energy of **L** induced by the three cations? Is the complexed cation fully shielded from solvent? Does it interact with the counterions?

The binding selectivity is another important issue. The simulations were undertaken four years ago before binding data were available in pure liquid solution. On the computational side, the representation of lanthanide and actinide cations in current force fields represents a challenging task[10]. Recently, parameters have been developed to fit the solvation free energies of M^{3+} ions in pure water solution,[11] following a methodology used for alkali and alkaline earth cations[12]. It is not clear whether these parameters depict the solvation properties in other liquid environments, or the interactions with anions and ligands. Thus, one important aspect of our work is to tentatively predict trends in binding affinities of **L** for the three lanthanides in a solvent where complexation can be investigated experimentally. For this purpose, we selected methanol as solvent. Another aspect deals with the mechanism of ion recognition by extractant molecules in liquid-liquid extraction or transport experiments. Based on molecular dynamics simulations, we recently pointed out the importance of interfacial phenomena in assisted cation extraction[13–20]. It was shown that ionophores in their free and complexed states behave as surfactants, while ions (and especially the highly charged ones) are repulsed by the interface. In the absence of experimental data on the surface activity of calixarene CMPO-like ligands, we decided to simulate typical LMX_3 complexes at

the water / chloroform interface in order to characterize their orientation with respect to the liquid phases, and to investigate the question of ion recognition at the interface.

We first describe the coordination of the three lanthanide ions by **L** in pure methanol solution and analyze some key interactions between the ions, the ligand, and the solvent(s). We then concentrate on the question of binding selectivity in pure methanol solution, which is also compared to aqueous solution. This is followed by simulations of the $Eu(NO_3)_3$ salt and its **L** complex at the water / chloroform interface, focusing on the question of ion recognition. Finally, we study the role of the calixarene platform in **L**. For this purpose we simulated the $(CMPO)_4$ "ligand", analogous of **L**, from which the calix[4]arene fragment was removed, at the water / chloroform interface.

METHODS

The molecular dynamics (MD) simulations were performed with the modified AMBER4.1 software[21] where the potential energy U is given by:

$$U = \Sigma_{bonds} K_r (r - r_{eq})^2 + \Sigma_{angles} K_\theta (\theta - \theta_{eq})^2 + \Sigma_{dihedrals} \Sigma_n V_n (1 + \cos n\phi) + \Sigma_{i<j} [q_i q_j / R_{ij} - 2\varepsilon_{ij} (R^*_{ij}/R_{ij})^6 + \varepsilon_{ij} (R^*_{ij}/R_{ij})^{12}]$$

The electrostatic and van der Waals interactions between atoms separated by at least three bonds are described within a pairwise additive scheme by a 1–6–12 potential. Parameters for the solutes were taken from the AMBER force field[22] and from previous studies on these molecules in pure homogeneous solvents. The atomic charges on **L** were fitted from ESP calculations of ref. [16] for the CMPO moieties and from ref. [23] for the calix[4]arene moiety. They were used without a special scaling factor for 1–4 interactions. The Lennard-Jones parameters of the La^{3+}, Eu^{3+} and Yb^{3+} cations (R^*_{La}= 2.105; R^*_{Eu} = 1.852; R^*_{Yb} = 1.656 Å; ε_{La} = 0.06; ε_{Eu} = 0.05; ε_{Yb} = 0.04 kcal/mol) have been fitted by Monte-Carlo simulations in order to reproduce their free energies of hydration[11]. Concerning the liquid phases, we used the TIP3P model for water[24] and the OPLS models for methanol and for chloroform [25]. A residue based 12 Å cut-off was applied to the non-bonded interactions where each ion and **L** were considered as single residues.

The simulated solvent systems are described in Table I. The water / chloroform interface (see Chart 2) has been built as indicated in ref.[26]. The LM^{3+} complexes were first minimized in the gas phase after 100 ps of MD, with the cation sitting in the pseudo-cavity delineated by the four phosphoryl O_p and the four carbonyl O_c oxygens. They were then immersed in solution. The NO_3^- or Cl^- counterions were initially placed in the second solvation sphere of the complex, at about 11 Å from M^{3+}, i.e. within the cut-off distance, and separated from LM^{3+} by one shell of solvent molecules.

Each solvent system was first energy minimized (1000 steps), then the solvent molecules were allowed to relax around the frozen solute during 50 ps of MD ("BELLY" option of AMBER). Next the free MD simulations were started with random velocities, and the temperature was maintained at 300 K by coupling to a thermal bath with a relaxation time of 0.2 ps. All C-H, O-H, H···H, C-Cl and Cl···Cl "bonds" were constrained with SHAKE, using a time step of 1 fs.

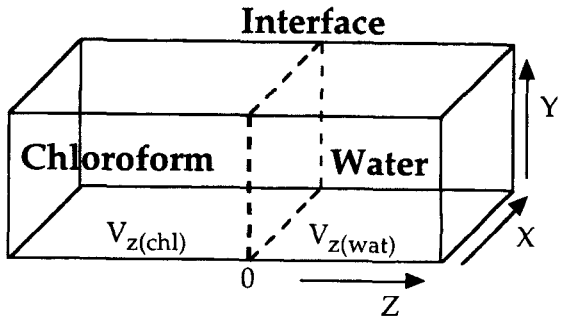

CHART 2 Schematic representation of the water/chloroform interface

TABLE I Simulation conditions for the different systems in methanol and at the water / chloroform interface

Solute		*nb methanol*	*nb chloro*	*nb water*	*box size* [a] $V_x \times V_y \times V_z$	*time* (*ns*)
Eu^{3+}		-	-	1083	32×32×32	0.11
		414	-	-	31×31×31	0.11
$Eu(NO_3)_3$		-	-	885	31×31×31	0.15
		555	-	-	34×34×34	0.12
$EuCl_3$		593	-	-	35×35×35	0.1
L		-	-	1213	35×35×35	0.35
		858	-	-	40×40×40	1.0
LM^{3+}		-	-	1320	36×36×36	0.2
$LM(NO_3)_3$		970	-	-	42×42×42	1.0
	b	-	248	716	28×28×(46+31)	0.36
	c	-	285	1512	34×34×(34+41)	1.0
$I \cdot MCl_3$		1036			42×42×42	1.0
$(CMPO)_4$		-	-	1514	38×38×38	0.1
		-	258	1197	36×31×(32+34)	0.8
$(CMPO)_4\ Eu(NO_3)_3$		-	-	1450	37×37×37	0.4
		-	245	1104	32×32×(33+34)	1.0
		597	-	-	36×36×36	1.6

a. For a water / chloroform interface the size of the box is: $V_x \times V_y \times (V_{z(chl)} + V_{z(wat)})$ (see Chart 2).
b. Simulations *a* to *c* with the NO_3^- anions in close contact with LM^{3+} (see section 2.1 of the text).
c. Simulation *a* with the NO_3^- counterions at about 8 Å from Eu^{3+}.

Binding selectivity: Free energy calculations

The change in free energy between two states (cations M_1^{3+} and M_0^{3+}) was calculated by using statistical perturbation theory, applying the windowing technique. The potential energy was defined as $U_\lambda = \lambda U_1 + (1-\lambda)U_0$, where U_1 and U_0 were calculated with the corresponding R_1^*, ε_1 and R_0^*, ε_0 parameters of the ions. At each window, the free energy differences between the states λ and $\lambda + \Delta\lambda$ ("forward calculation") and between the states λ and $\lambda - \Delta\lambda$ ("backward calculation") were obtained by:

$$\Delta G_{\lambda_i} =$$

$$G_{\lambda_{i+1}} - G_{\lambda_i} = -R\,T \ln \left\langle \exp^{-\frac{U_{\lambda_{i+1}} - U_{\lambda_i}}{R\,T}} \right\rangle_{\lambda_i}$$

where R is the molar gas constant and T is the absolute temperature. $\langle\rangle_{\lambda i}$ stands for the ensemble average at the state λ_i where $U_{\lambda i}$ is the potential energy. Details are given in the text and in Tables IV–VI.

Analysis of results

Average structural features and energy components were analyzed from the trajectories saved every 0.2 ps using the MDS and DRAW software[27]. The position of the liquid-liquid interface was recalculated at each step as the intersection of the density curves of the solvents, as described in ref.[13].

The interaction energies between the different groups (cation, anion, ligand) and each solvent were recalculated from the trajectories.

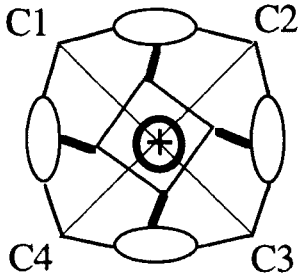

CHART 3 Schematic representation of C_4 arrangement of the cone with the four P=O groups (thick lines) of the LM^{3+} complexes

RESULTS

1- The uncomplexed ligand L and its LMX_3 complexes in methanol

Average structural parameters of free and complexed ligand **L** are reported in Table II.

TABLE II Structural features of the LMX_3 complexes in methanol. Average distances (Å), angles (°) and fluctuations in the last 100 ps of the simulation

X^- / M^{3+}	[a]	NO_3^-			Cl^-		
		La^{3+}	Eu^{3+}	Yb^{3+}	La^{3+}	Eu^{3+}	Yb^{3+}
$<\omega_{13}>$	165 ± 5	133 ± 4	142 ± 4	140 ± 3	140 ± 3	140 ± 6	142 ± 2
$<\omega_{24}>$	103 ± 7	144 ± 4	138 ± 3	140 ± 4	136 ± 4	142 ± 4	142 ± 4
$dC_1\cdots C_3$	7.4 ± 0.2	7.3 ± 0.2	7.3 ± 0.2	7.4 ± 0.2	7.3 ± 0.2	7.3 ± 0.2	7.3 ± 0.1
$dC_2\cdots C_4$	7.2 ± 0.2	7.3 ± 0.2	7.3 ± 0.2	7.2 ± 0.2	7.2 ± 0.2	7.3 ± 0.2	7.3 ± 0.1
$dM\cdots O_p$	3.2 ± 0.6 [b]	2.5 ± 0.1	2.3 ± 0.1	2.2 ± 0.1	2.6 ± 0.1	2.3 ± 0.1	2.2 ± 0.1
	7.4 ± 0.4 [b]						
CN_{Op} [c]		4	4	4	4	4	4
$dM\cdots O_c$	4.3 ± 0.6 [b]	2.8 ± 0.5	2.6 ± 0.1	2.5 ± 0.1	2.8 ± 0.2	2.5 ± 0.1	2.4 ± 0.1
	6.7 ± 0.6 [b]		4.6 ± 0.3	3.8 ± 0.2	3.5 ± 0.5	3.7 ± 0.4	
CN_{Oc} [c]		4	3	3	3	3	4
			1	1	1	1	
$dM\cdots X$	–		3.5 ± 0.1		7.3 ± 0.6	8.0 ± 0.5	8.3 ± 0.5
		8.9 ± 0.8	8.6 ± 0.8	8.2 ± 0.5	27 ± 2	19 ± 3	20 ± 1
nb_X [d]			1		1	2	1
		3	2	3	2	1	2
$dM\cdots O_m$	–	2.7	4.0	2.7	2.8	–	–
CN_{Om} [c]		1	1	1	1		
Total M^{3+} CN [e]	–	9	8	8–9	8–9	7–8	8
nb $NH\cdots X^-$ / O_m [f]	–	1/3	1/3	0/4	1/3	1/3	0/4

a. Uncomplexed ligand **L**.
b. Distance between the oxygen and the"C4" symmetry axis of the cone.
c. Number of O_p / O_c atoms of **L**, or of O_m atoms of methanol, coordinated to M^{3+}.
d. Number of X^- anions situated at the distances given above.
e. Coordination number of M^{3+}, estimated by counting its nearest neighbors on the basis of CN_{Op}, CN_{Oc}, CN_{Om} and nb_X.
f. Number of X^- anion / $O_{methanol}$ atoms hydrogen bonded to the N-H groups of **L**.

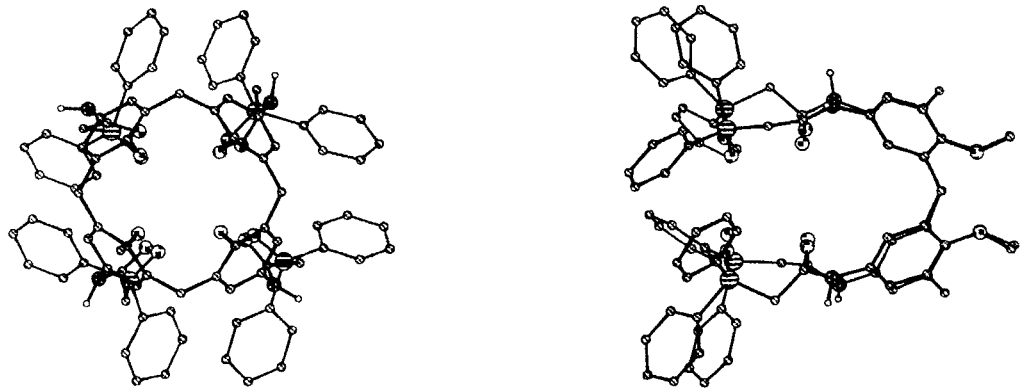

Free ligand L (0 ps)

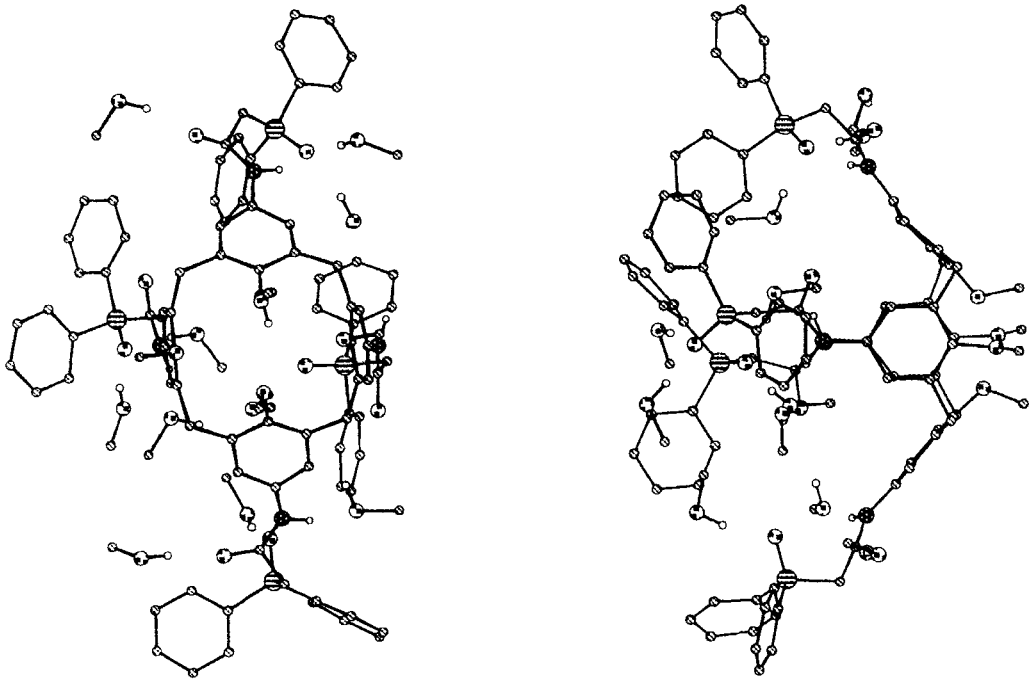

Free ligand L (1 ns)

FIGURE 1 Snapshot of the free ligand L in methanol at 0 ps and 1 ns (orthogonal views)

1.1- The free ligand L

In order to gain insights on the influence of the cation on the ligand conformation, we simulated the uncomplexed ligand **L** in methanol solution. The simulation started with a "closed" conformation of C_4 symmetry, extracted from the Eu^{3+} complex (*vide infra*), i.e. with converging O_p and O_c oxygens of the CMPO arms (Figure 1 and

Chart 1). During the simulation, the pseudo-cavity opened smoothly, as some CMPO arms rotated, leading to unsymmetrical "open" arrangements. The distances between the O_p and O_c atoms and the symmetry axis of the cone ranged from 2.6 to 7.8 Å. The O_p and O_c oxygens formed hydrogen bonds with methanol molecules, while other solvent molecules moved inside the cone of **L**. After 0.5 ns, the conformation of **L** remained nearly unchanged until the end of the simulation (1 ns). The cone moiety was of about C_2 symmetry, with two opposite phenyl rings being nearly parallel ($\omega_{13} = 165°$) and two others nearly perpendicular ($\omega_{24} = 103°$). The $C_1 \cdots C_3$ and $C_2 \cdots C_4$ distances between opposite CH_2 connectors fluctuated between 7.0 and 7.6 Å (see Chart 1 and Table II). The energy component analysis shows that the stabilization of **L**, with respect to the initial "closed" form, results mainly from its solvation energy ($\Delta = -180$ kcal/mol).

1.2 – Structural features of the LMX_3 complexes

The simulations of all M^{3+} complexes in methanol start with an inclusive form (M^{3+} surrounded by the four CMPO arms), where the three X-counterions ($X^- = NO_3^-$ / Cl^-) are placed in the equatorial plane (perpendicular to the symmetry axis) as shown in Figure 2.

During the whole simulation (1 ns), all complexes remain of inclusive type, with the M^{3+} ion surrounded by four phosphoryl oxygens and three to four carbonyls of the ligand. On the average, the cone formed by the four aromatic groups displays a C_{4v} symmetry, with the cation sitting on the symmetry axis: the ω_{13} and ω_{24} angles between the planes formed by two opposite aromatic rings are about 140 ± 4°, and the crossed $C_1 \cdots C_3$ and $C_2 \cdots C_4$ distances are equal (7.3 ± 0.2 Å). However, taking into account the four CMPO arms leads to a lower symmetry. Indeed the four phosphoryl groups display a fairly rigid squared arrangement, that is skewed with respect to the cone, as schematized in Chart 3. On the average, the four carbonyls are not of C_4 symmetry, because of their high mobility. The two types of counterions display different behaviors. None of the Cl^- anions are directly coordinated to M^{3+}. The closest ones, at about 8 Å from M^{3+}, are hydrogen bonded to one or two N-H protons, while the others have moved to the "bulk" solvent. The NO_3^- anions are generally closer from M^{3+} than the Cl^- ones (Figure 3 and Table II), two of them being in an "equatorial" position (hydrogen bonded to the N-H protons) and the third one "axial" (near the C_4 symmetry axis). In the case of the LEu^{3+} complex, one NO_3^- has migrated into the first coordination sphere of the cation. The N-H protons of **L** are thus hydrogen bonded to counterions or to solvent molecules.

The coordination number CN of the complexed cation, initially equal to 8 ($4O_p + 4O_c$ oxygens of **L**) increased to about 9 during some of the simulations. Schematically, two types of octa-coordination are observed. Details are given in Table II. In the $LEuCl_3$ and $LYbCl_3$ complexes, the cation is surrounded by the eight ligand oxygens as in the starting structures. This binding mode differs from the one found in the $LEu(NO_3)_3$ complex where one NO_3^- anion is bound to the cation, while a carbonyl group has moved out of the coordination sphere of Eu^{3+}. In the case of a nona-coordinated M^{3+} (in the two $LLaX_3$ and in the $LYb(NO_3)_3$ complexes), one methanol molecule is bound to the cation. However, in several cases, due to fluctuating binding of some carbonyl groups to M^{3+}, the CN cannot be precisely defined. For instance, in the $LYb(NO_3)_3$ complex, the CN is either 8 or 9, depending on the way one counts the carbonyl oxygen which is on the average at 3.8 Å. Similarly, in the $LEu(NO_3)_3$ complex, where the CN of Eu^{3+} is 8, one finds an additional solvent molecule at 4.0 Å from Eu^{3+}, between M^{3+} and one axial NO_3^-. In all complexes, we notice that the phenyl substituents of the CMPO arms are not equivalent. Schematically, four of them are "equatorial", and the four others are "axial", shielding the complexed cation from the envi-

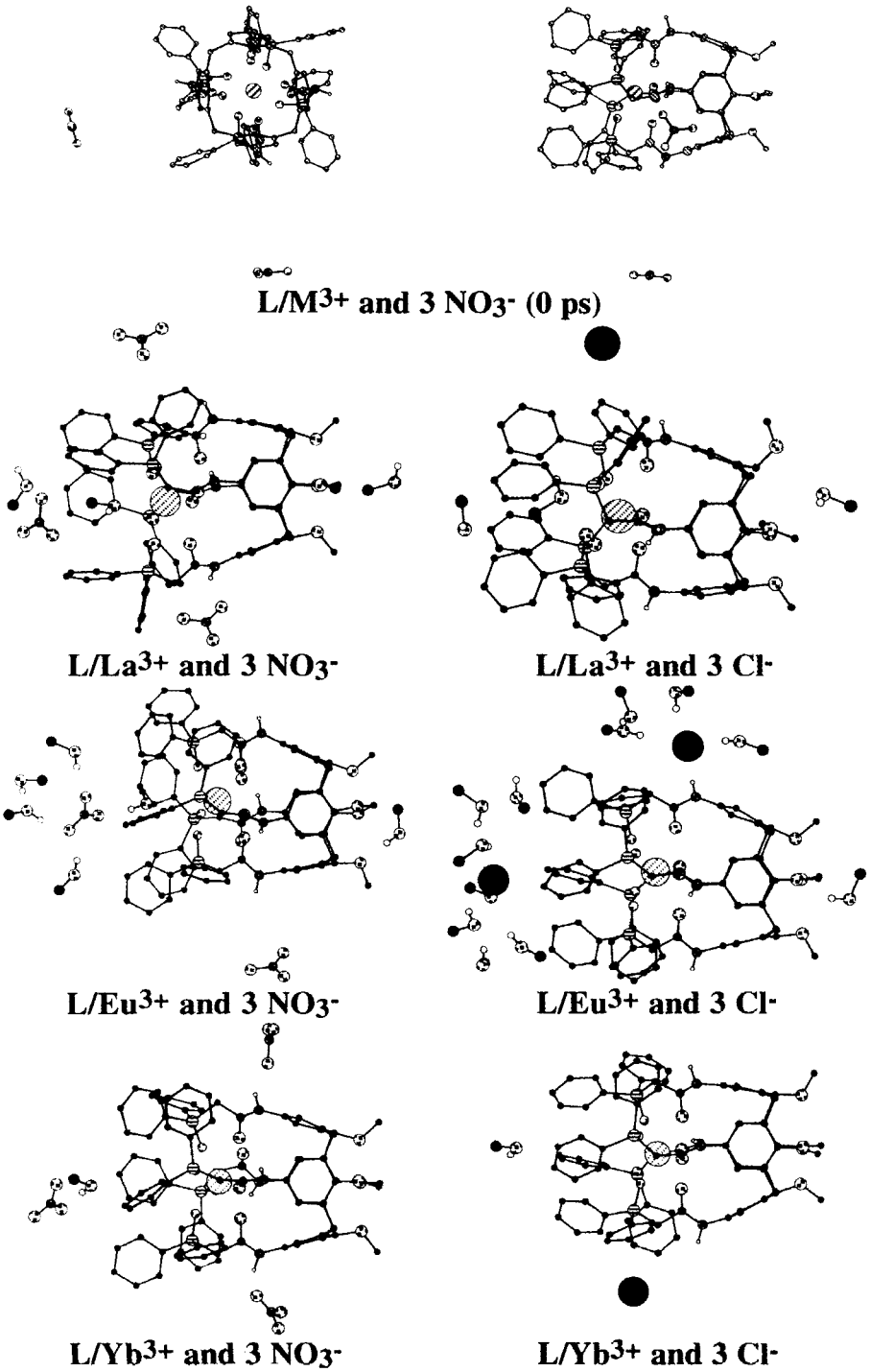

FIGURE 2 Snapshot of the LMX_3 complex at 0 ps (top ; orthogonal views), and of the $L{\cdot}M(NO_3)_3$ (*left*) and $LMCl_3$ (*right*) complexes (M = La, Eu and Yb) in methanol solution at 1 ns

ronment (Figure 2). However, important distorsions are found, related to the asymmetric binding of the carbonyls.

For a given cation, the four $M^{3+}\cdots O_p$ distances are nearly identical (see Table II). They decrease with the size of the cation (from about 2.6 to 2.2 Å, with the two types of counterions), as expected. The same trend is found for those $M^{3+}\cdots O_c$ distances which involve direct coordination to M^{3+}(from 2.8 to 2.4 Å). Thus, a given cation is somewhat closer to the O_p than to the O_c oxygens (by 0.2 to 0.3 Å on the average). In addition, as noticed above, some $M^{3+}\cdots O_c$ distances are quite large, when the carbonyls are loosely coordinated to Eu^{3+} (at ≈ 3.7 Å in $\mathbf{L}EuCl_3$) or "diverging" (at ≈ 4.6 Å in $\mathbf{L}Eu(NO_3)_3$). The latter case corresponds to an exchange with a nitrate counterion which becomes coordinated to the cation (monodentate binding). It is the only case where a counterion was found to be bound to an octa-coordinated cation.

All complexes display dynamic features. The cone of the calixarene is not instantaneously of C_{4v} symmetry: the ω_{13} and ω_{24} angles between opposite aromatics oscillate between 133 and 142°, while the $C_1\cdots C_3$ and $C_2\cdots C_4$ distances fluctuate between 7.0 and 7.6 Å. As illustrated in Figure 4, the motions are anticorrelated, leading to structures of approximate C_2 symmetry. We notice that, instantaneously, the cation sits away from the "symmetry axis". In a given complex, the $M^{3+}\cdots O_p$ distances are nearly constant during the dynamics, while some $M^{3+}\cdots O_c$ ones vary by up to 3 Å (Figure 3), corresponding to torsions of the CMPO arms and to large fluctuations of axial / equatorial $OP(Ph)_2$ groups. Compared to the free ligand, the cone of the complexed **L** is more C_{4v}-like. It is, on the average, somewhat less symmetrical in the La^{3+} than in the Yb^{3+} complexes (see ω_{13} and ω_{24}angles in Table II).

1.3 – *Energy characteristics of the LMX_3 complexes*

The energy component analysis (Table III) shows that the interaction between **L** and M^{3+} is quite large (from 720 to 940 kcal/mol) and increases markedly from La^{3+} to Yb^{3+} (by about 180 kcal/mol in the $\mathbf{L}M(NO_3)_3$ complexes, and by 220 kcal/mol in the $\mathbf{L}MCl_3$ ones). There are thus counterion effects on the cation···ligand interactions. The latter are reduced when counterions bind to M^{3+}. The complexation induces significant strain in the ligand, whose internal energy increases by about 190 kcal/mol upon complexation of $La(NO_3)_3$ or $LaCl_3$. Futhermore, the internal energy of **L** is about 40 kcal/mol higher in the $Yb(NO_3)_3$ complex, and 70 kcal/mol higher in the $YbCl_3$ complex, than in the corresponding La^{3+} complexes. In relation with the different binding modes of the X^- counterions, we note that the interactions of M^{3+} with the three nitrates are more attractive (about –100 to -130 kcal/mol per NO_3^-) than those with the chlorides (which range from –113 kcal/mol when Cl^- is in the second coordination sphere of M^{3+}, to zero when Cl^- has moved beyond the cutoff distance from M^{3+}). The interactions between the anions and **L** are comparatively weak. They are attractive (up to about 10 kcal/mol) when X^- is hydrogen bonded to **L**, and repulsive when X^- is coordinated to M^{3+}.

In all cases, the complexed cation, although well shielded by **L**, displays attractive interactions with methanol (from –126 to –267 kcal/mol). These interactions are somewhat larger with Cl^- than with NO_3^- counterions, in relation with the competitive binding of the latter to M^{3+}. The attractions are largest with La^{3+}, to which one solvent molecule is directly coordinated. The solvation of the complexed ligand **L** itself also leads to attractive interactions (about –110 to –160 kcal/mol), but no systematic trends can be found, due to the interplay between the cation, **L**, counterion and solvent interactions. It is thus anticipated that the binding selectivity of **L** for a given cation in solution cannot solely be assessed from the interactions between **L** and the cation. This is why we have undertaken free energy perturbation simulations (see next) to address this important question.

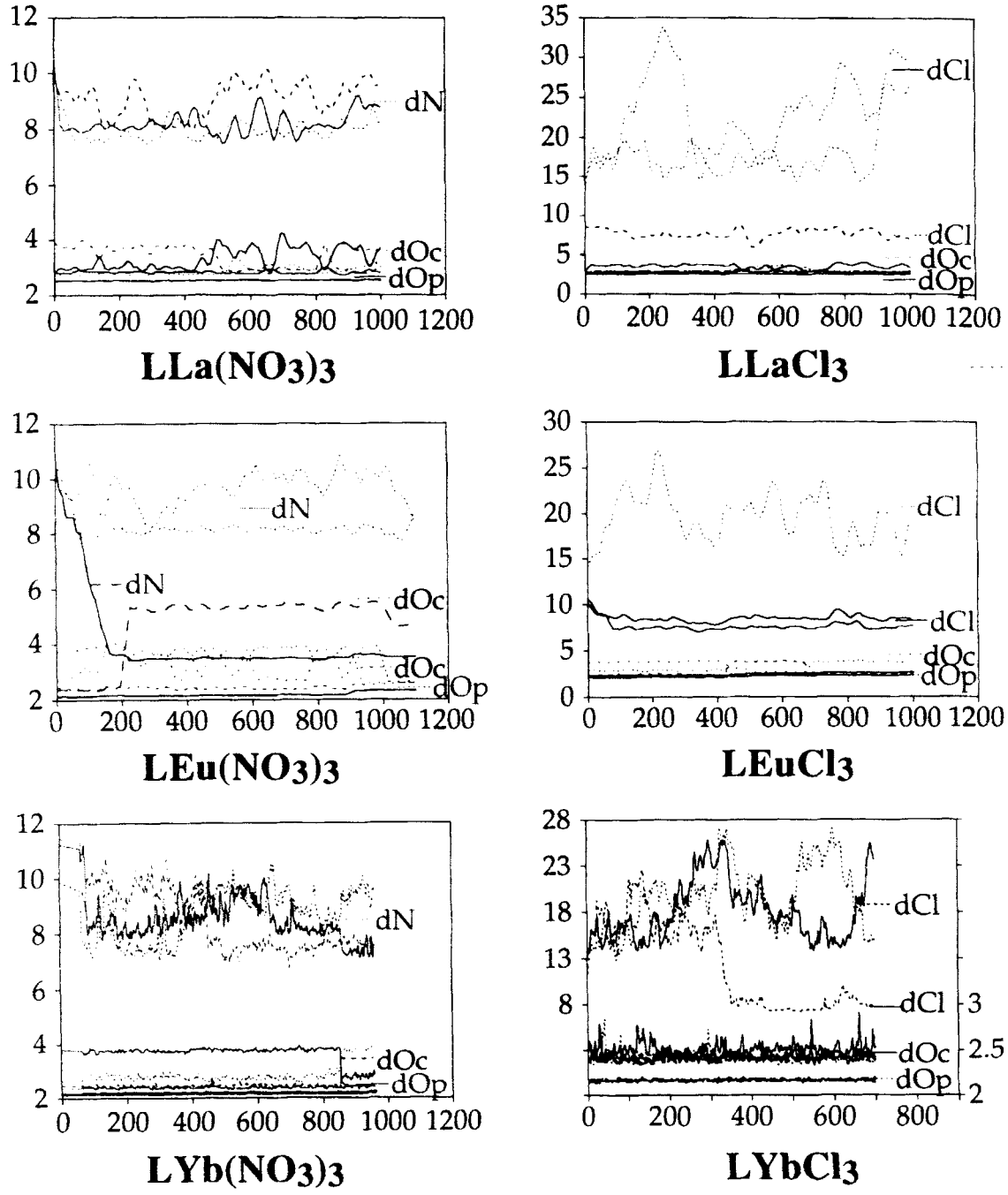

FIGURE 3 LMX_3 complexes in methanol solution: distances (Å) between M^{3+} and O_p, O_c oxygens of L, between M^{3+} and N_{NO3^-} or Cl^- as a function of time (ps)

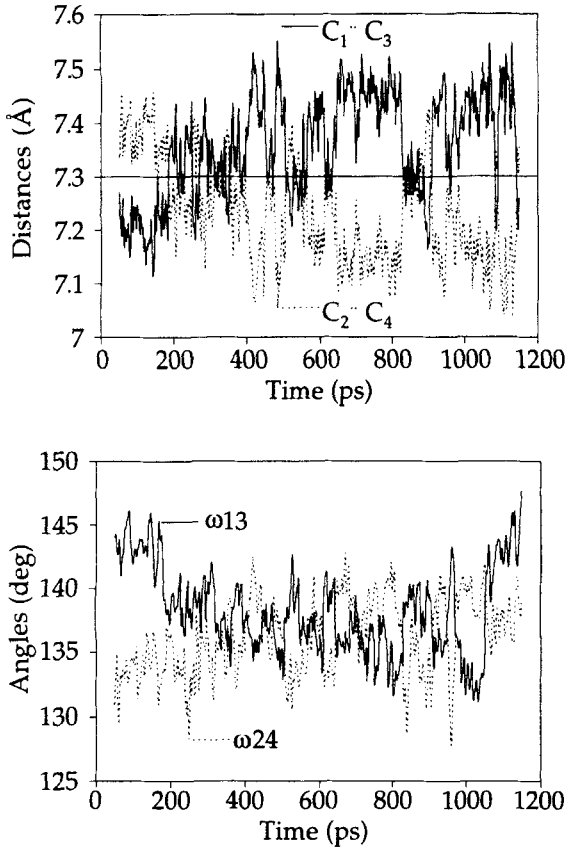

FIGURE 4 The $LEu(NO_3)_3$ complex in methanol. Distances $C_1 \cdots C_3$ and $C_2 \cdots C_4$ between opposite CH_2 groups (see Chart 3), and angles between opposite aromatic rings of L as a function of time

1.4 – *Cation recognition by L in methanol*

We have performed FEP simulations in order to assess the binding selectivity of the calixarene L for the La^{3+} / Eu^{3+} / Yb^{3+}cations in methanol solution. For most studies, nitrates were selected as counterions, but we also considered the uncomplexed salts with Cl^- as counterions, and the LM^{3+} complexes without counterions. For the purpose of comparison between the methanol and aqueous solutions, we have repeated these simulations in water (see Table IV).

The binding selectivity of L ("Calix") for M_1^{3+} *vs* M_2^{3+} cations is defined by $\Delta\Delta G = \Delta G_2 - \Delta G_1$. According to the thermodynamic cycle shown in Scheme 1, $\Delta\Delta G$ is also equal to $\Delta G_4 - \Delta G_3$, where ΔG_3 and ΔG_4 correspond to the mutations of the M_1^{3+} to the M_2^{3+} cations in solution, respectively in their uncomplexed and complexed states ("computational alchemy"[28,29]).

$$\begin{array}{ccc} Calix + M_1^{3+} & \xrightarrow{\Delta G_1} & Calix\,/\,M_1^{3+} \\ \Delta G_3 \downarrow & & \downarrow \Delta G_4 \\ Calix + M_2^{3+} & \xrightarrow{\Delta G_2} & Calix\,/\,M_2^{3+} \end{array}$$

SCHEME 1

The calculation of ΔG_4 and ΔG_3 started respectively from the $LEu(NO_3)_3$ complex after 1 ns of MD, and from the $Eu(NO_3)_3$ salt, after 100 ps of MD simulation. Eu^{3+} was mutated into La^{3+} and into Yb^{3+}.

We first checked that using this protocol for the uncomplexed M^{3+} cations in water (no counterions) leads to ΔG_3 values which are close to those obtained by Monte Carlo simulations (57.2 *vs* 56.1 kcal/mol for the $Eu^{3+} \rightarrow La^{3+}$ions, and –46.5 *vs* –44.9 kcal/mol for the $Eu^{3+} \rightarrow Yb^{3+}$ ions)[11], and in reasonable agreement with the experimental values[30] (Table IV).

In methanol solution, the counterions were taken into account for the mutations, as the uncomplexed salts are less dissociated than in water[31]. We thus compare the MCl_3 and $M(NO_3)_3$ salts forming intimate ion pairs. During the simulations, both types of salts remained bound. Thus we calculated ΔG_3 for three typical situations: with the intimate nitrate *vs* chloride ion pairs (no dissociation), and with the completely solvated M^{3+} cations (no counterion), corresponding to the hypothetical case where the salts are fully dissociated. In the latter case, the ΔG_3 values are found to be somewhat smaller in methanol than in water (45.5 kcal/mol for $Eu^{3+} \rightarrow La^{3+}$ and –37.3 kcal/mol for $Eu^{3+} \rightarrow Yb^{3+}$), as expected from the poorer coordination properties of methanol, compared to water. In the presence of either NO_3^- or Cl^- counterions,

the ΔG_3 energies are similar, and larger than in the absence of counterions (Table IV). Table IV also shows that the total coordination number (CN) of the uncomplexed M^{3+} cations depends on the solvent and on the counterion. From La^{3+} to Yb^{3+} (no counterion) CN ranges from 10 to 9 in water, and from 9 to 8 in methanol. Our calculated CN's in water are somewhat larger than those reported by Merbach *et al.* using improved treatments of non-covalent interactions[32]. In methanol, the NO_3^- counterions bind M^{3+} in a monodentate mode, leading to CN's from 10 to 8. The Cl^- anions, which are more bulky than the oxygen atoms of the NO_3^- anions, are found to lead to lower CN's (from 8 to 7).

The calculation of the ΔG_4 free energies in methanol, performed on the $LM(NO_3)_3$ complexes, leads to values somewhat more negative than the corresponding ΔG_3 ones (64.3 kcal/mol for the $Eu^{3+} \rightarrow La^{3+}$ mutation, and -51.6 kcal/mol for the $Eu^{3+} \rightarrow Yb^{3+}$mutation). As a result, the ΔG_4- ΔG_3 values are negative, indicating that complexation of the smallest cation is preferred, *i.e.* the binding strength in methanol decreases in the order $Yb^{3+} > Eu^{3+} > La^{3+}$.

Although **L** and its complexes are not soluble in water, we repeated the calculations of ΔG_4 in this solvent, in order to get some insight into the role of the solvent on the binding selectivity. These calculations were performed without counterions, as water is more dissociating than methanol. It can be seen from Table IV that the ΔG_4 energies in water are close to those in methanol, but somewhat larger. This likely results from the fact that in methanol solution, one NO_3^- anion is coordinated to the complexed cation, while in water this anion is replaced by two water molecules coordinated to M^{3+}. These interactions lead to the same sequence of binding selectivities in the two solvents, *i.e.* Yb^{3+} better complexed than Eu^{3+} and than La^{3+}. According to this analysis, the selectivity follows the order of interactions between the cation and **L**, instead of the cation desolvation energies (which would favor La^{3+} over Yb^{3+}). This thus suggests that the binding sequence should remain similar in another solvent environment, as shown below for the water / chloroform interface.

TABLE III Energy component analysis of the **L**·MX_3 complexes in methanol. Averages over the last 100 ps of the simulation

$X^- M^{3+}$	[a]	NO_3^-			Cl^-		
		La^{3+}	Eu^{3+}	Yb^{3+}	La^{3+}	Eu^{3+}	Yb^{3+}
L	−380 ± 11	−190 ± 13	−205 ± 16	−152 ± 14	−194 ± 14	−158 ± 13	−125 ± 12
L/solvent	−349 ± 16	−108 ± 15	−140 ± 12	−128 ± 10	−127 ± 14	−140 ± 13	−159 ± 9
L/M^{3+}	-	−721 ± 14	−755 ± 19	−903 ± 12	−724 ± 13	−837 ± 16	−942 ± 10
L/X^-	-	-3 ± 6	−8 ± 8	−9 ± 4	0 ± 1	−6 ± 8	−1 ± 4
		2 ± 7	49 ± 7	−6 ± 5	11 ± 8	−10 ± 3	−2 ± 3
		−13 ± 7	−1 ± 13	−5 ± 7	0 ± 0	−1 ± 2	−0 ± 3
M^{3+}/solvent	-	−233 ± 31	−126 ± 36	−191 ± 16	−267 ± 14	−189 ± 29	−209 ± 17
M^{3+}/X^-	-	−114 ± 8	−116 ± 12	−130 ± 4	0 ± 0	−118 ± 6	−119 ± 10
		−105 ± 7	−297 ± 5	−105 ± 5	−138 ± 12	−133 ± 4	0 ± 0
		−124 ± 7	−110 ± 17	−135 ± 7	0 ± 0	0 ± 0	0 ± 0
X^-/solvent	-	−79 ± 12	−81 ± 18	−65 ± 10	−68 ± 21	−67 ± 10	−72 ± 13
		−97 ± 13	13 ± 9	−90 ± 10	−60 ± 12	−54 ± 9	−95 ± 19
		−61 ± 14	−87 ± 13	−57 ± 12	−68 ± 16	−96 ± 18	−107 ± 19
LMX_3	-	−1269 ± 15	−1379 ± 19	−1390 ± 12	−1045 ± 14	−1263 ± 16	−1189 ± 12
LM^{3+}	-	−911 ± 15	−960 ± 19	−1055 ± 14	−918 ± 14	−995 ± 16	−1067 ± 12

a. Uncomplexed ligand **L**.

TABLE IV Energy results (kcal/mol) of the FEP simulations on the M^{3+} cations and on their complexes in water and methanol solutions

	In water [a]		*In methanol* [a]	
	$La^{3+} \rightarrow Eu^{3+}$	$Eu^{3+} \rightarrow Yb^{3+}$	$La^{3+} \rightarrow Eu^{3+}$	$Eu^{3+} \rightarrow Yb^{3+}$
ΔG_3 (M^{3+})	−57.2 ± 0.3	−46.5 ± 0.1	−45.5 ± 0.1	−37.3 ± 0.1
CN[b]	10 → 9	9 → 9	9 → 9	9 → 8
ΔG_3 ($M(NO_3)_3$)	–	–	−56.6 ± 0.1	−44.3 ± 0.1
CN[b]	–	–	10 → 9	9 → 8
ΔG_3 (MCl_3)	–	–	−54.6 ± 0.1	−44.6 ± 0.1
CN[b]	–	–	8 → 7	7 → 7
ΔG_3 (M^{3+})[c]	−56.1	−44.9	–	–
ΔG_3 (exp)[d]	−51.4	−50.0	–	–
ΔG_4 (LM^{3+})	−69.7 ± 0.2	−56.8 ± 0.1	–	–
CN[b]	9 → 8	8 → 9		
ΔG_4 ($LM(NO_3)_3$)	–	–	−64.3 ± 0.1	−51.6 ± 0.1
CN[b]			9 → 9	9 → 9
$\Delta\Delta G$ (LM^{3+})[e]	−12.5	−10.3		
$\Delta\Delta G$ ($LM(NO_3)_3$)[e]	–	–	−7.7	−7.3

a. Mutation performed in 50 windows (2 + 3 ps) with a twin cutoff (11/15Å).
b. Average Coordination Number at the beginning and at the end of the mutation.
c. From ref[11].
d. After Marcus[30].
e. $\Delta\Delta G = \Delta G_4 - \Delta G_3$. See scheme I.

2- The L·Eu$(NO_3)_3$ complex and Eu$(NO_3)_3$salt at the water / chloroform interface

In relation with the detailed mechanistic issues of ion capture and extraction by **L**, we simulated typical LMX_3 complexes at a water / chloroform interface, in order to first assess to which extent they are surface active, and whether they adopt a specific position and orientation with respect to the interface. A second issue concerns the question of ion recognition (binding selectivity) *at the interface*[33]. This is addressed by FEP calculations, similar to those reported above in bulk water and methanol solutions.

2.1 – The calixarene complexes adsorb at the interface

We simulated the L$Eu(NO_3)_3$ complex at the interface, starting with three different positions *a* to *c* (Figure 5) with the C_4 symmetry axis of **L** perpendicular to the interface. Orientation *a* is the one expected after a least motion uptake of the cation from water by **L**: the complexation site (Eu^{3+} and the four CMPO's) sits on the water side of the interface, while the OMe groups at the lower rim point to chloroform. Orientations *b* and *c* are inverted, relative to *a*: their cationic site is oriented towards the chloroform phase. The only difference between *b* and *c* concerns the penetration depth of the complex in the chlorofom phase: in *b*, the Eu^{3+} cation sits right at the interface, while in *c*, it sits more deeply in chloroform, at about 8 Å from the interface. The latter situation would thus correspond to a nearly extracted complex and we wanted to test whether the extraction would proceed further to the organic phase. In *a* to *c*, the initial structure of the complex is taken from a simulation in water where two nitrates coordinate

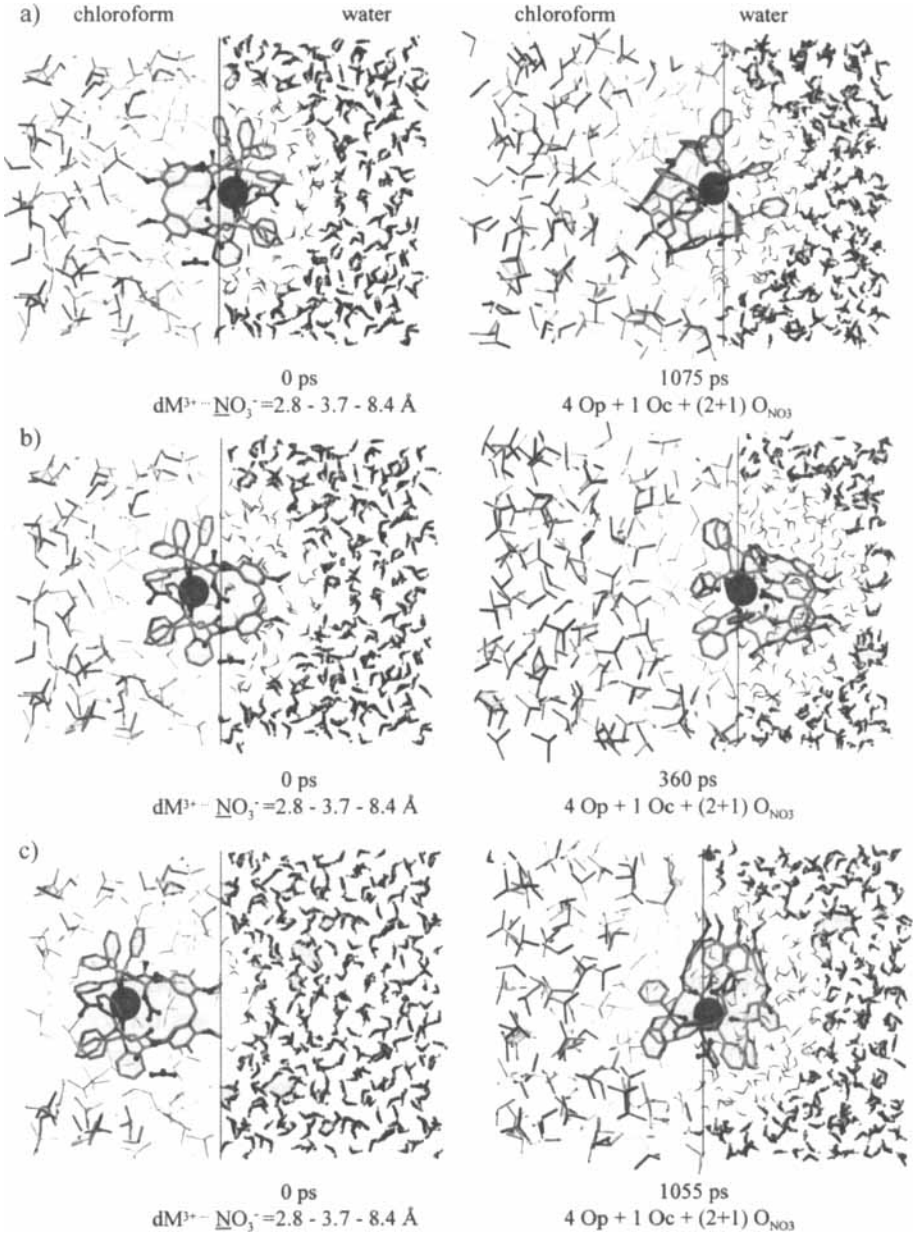

FIGURE 5 Snapshots of the **L**Eu$(NO_3)_3$ complex at the water / chloroform interface, with three different initial (left) and final (right) positions: a to c. Initial $M^{3+} \cdots N_{NO3^-}$ distances (*left*) and final coordination sphere of Eu^{3+} (*right*). The solvent molecules around the solute are displayed differently from those of "the bulk" for clarity (See Color Plate I at the back of this issue)

to the cation, and the third one is "*exo*", in the equatorial plane of **L**. We selected this structure, which is likely less hydrophilic than with fully dissociated counterions, in order to facilitate its extraction.

TABLE V Energy results (kcal/mol) of the FEP simulations on the M^{3+} complexes at the water / chloroform interface [a]

Starting conformation	*2 NO_3^- coordinated to M^{3+}* [b]		*1 NO_3^- coordinated to M^{3+}* [c]	
	$La^{3+} \rightarrow Eu^{3+}$	$Eu^{3+} \rightarrow Yb^{3+}$	$La^{3+} \rightarrow Eu^{3+}$	$Eu^{3+} \rightarrow Yb^{3+}$
$\Delta G_{4\text{-itf}}$ ($LM(NO_3)_3$)	−75.9 ± 0.8	−64.2 ± 0.1	−66.2 ± 0.1	−54.4 ± 0.1
CN[d]	9 → 9	9 → 9	9 → 9	9 → 8
$\Delta\Delta G$ ($LM(NO_3)_3$)[e]	−18.7	−17.7	−9.0	−7.9

a. Mutation performed in 20 windows (of 2 + 3 ps each) with a 12Å cutoff.
b. The solvent box contains 228 $CHCl_3$ + 766 H_2O molecules; its size is 28×28×(44+31)Å^3.
c. 285 $CHCl_3$ + 716 H_2O molecules; size 28×28×(46+31)Å^3.
d. Average Coordination Number calculated after at least 100 ps of free MD at the beginning and at the end of the mutation.
e. $\Delta\Delta G = \Delta G_{4\text{-itf}} - \Delta G_{3\text{-wat}}$; see Scheme 2

In fact, in none of the simulations, did the complex migrate to the organic phase. It either remained adsorbed at the interface or returned to it, adopting different orientations and Eu^{3+} positions with respect to the interface. In cases *a* and *b*, the calixarene **L** was still more or less perpendicular to the interface, while in case *c*, it was rather parallel (Figure 5). In the three cases, the Eu^{3+} cation was right at the interface (Figure 5). There is thus no unique orientation of the complex, in relation with the weak differences in electrophilicity / hydrophobicity of its different moieties. Indeed, the eight phenyl groups of the CMPO's, which prevent hydration of the cationic site at the upper rim, as well as the calixarene moiety, are hydrophobic. In another simulation, we attempted to model the $Eu(NO_3)_3$ complex of an analogue of **L** where the four OMe groups at the lower rim were replaced by more hydrophobic OPhenyl groups. During 1 ns of MD, starting with the C_4 symmetry axis of the complex in the plane of the interface, the complex retained the same orientation, presumably because of its low amphiphilicity. This behavior contrasts indeed with the one of smaller molecules like TBP (tri-*n*-butyl-phosphate) which reorients at the interface in less than 100 ps[19].

The lack of clear-cut orientation of **L** at the interface indirectly points out the importance of O-alkyl substituents at the lower rim[5,6]. Experimentally, the extraction of Eu^{3+} by **L** derivatives has been found to increase from O-C_5H_{11} to O-$C_{14}H_{29}$, and then to decrease when the alkyl chains become longer [5]. Such substituents rigidify the cone. They also modulate the amphiphilicity of the extractant and its orientation at the interface. The CMPO's should sit on the water side of the interface to facilitate the cation capture via a least motion pathway.

In all three simulations the complexes remained of inclusive type at the interface, with Eu^{3+} coordinated to the four O_p oxygens (at 2.1 – 2.2 Å), and to one O_c oxygen only (at 2.5 – 3.6 Å). The other carbonyls adopted diverging orientations (at 4.5 – 6.6 Å from Eu^{3+}). The coordination number of Eu^{3+} was eight, involving 4 O_p, 1 O_c and (2+1) O_{NO3} oxygens. The cation was thus completely shielded from the solvents while the uncoordinated O_c oxygens were hydrogen bonded to water molecules. The uncoordinated nitrate either stayed at the interface or migrated to the bulk water.

We checked that the status of NO_3^- counterions does not critically determine the interfacial behaviour of the LEu^{3+} complex by performing another simulation, where the three anions were initially somewhat more remote from Eu^{3+} (at about 6 Å), and the complex in position *a*. After 1 ns, one NO_3^- had entered the first coordination sphere of Eu^{3+}, while the two others remained in water, within 10 Å from Eu^{3+}. The orientation of the complex was, however, similar to the one obtained in simulation *a*, confirming its surface activity.

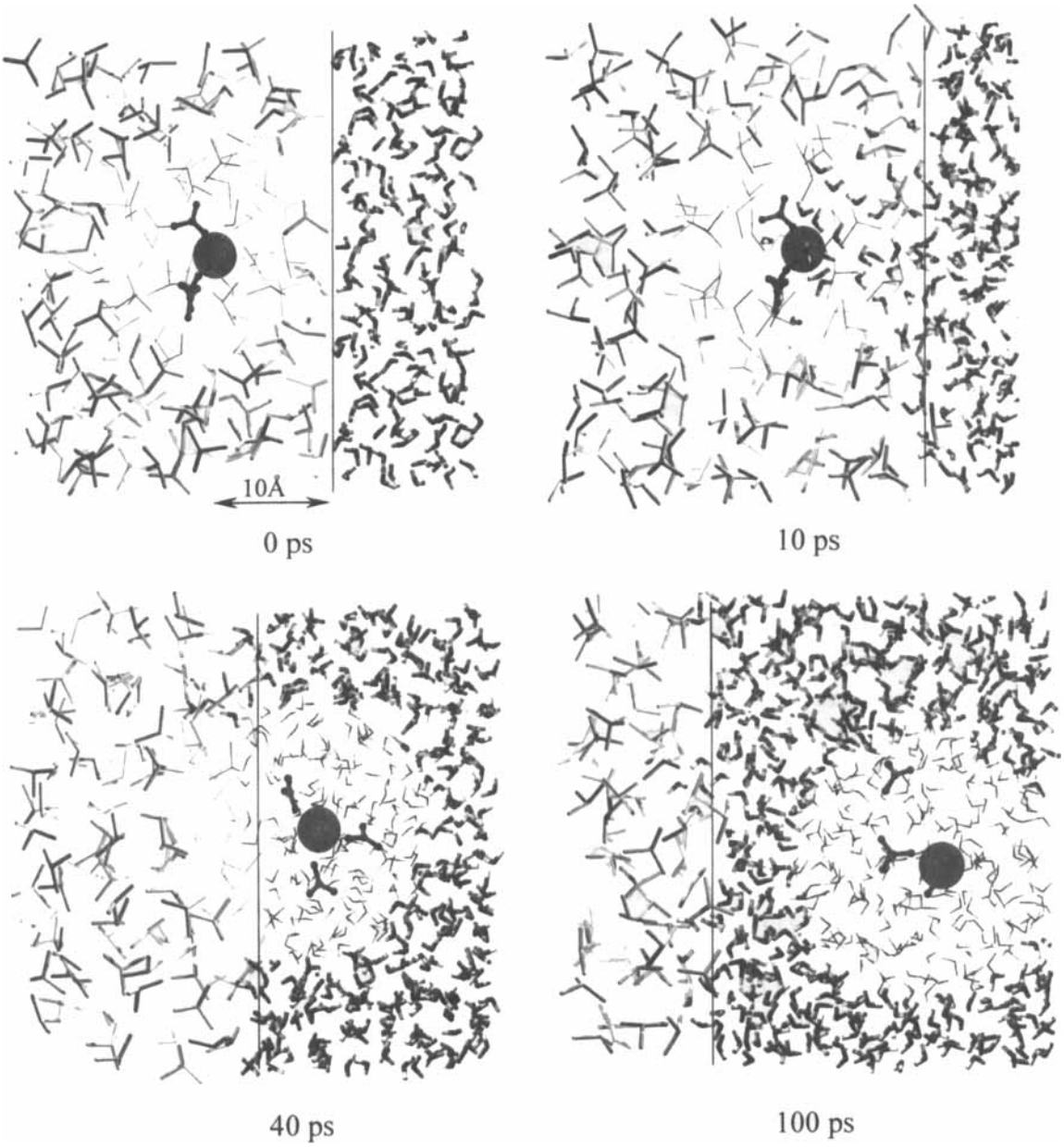

FIGURE 6 Snapshots of the $Eu(NO_3)_3$ salt at the water / chloroform interface, initially in chloroform (0 ps). The solvent molecules around the solute are displayed differently from those of "the bulk" for clarity (See Color Plate II at the back of this issue)

2.2 – *The uncomplexed salt is "repelled" by the interface*

The crucial role of complexation on the interfacial activity was evidenced by a simulation of the uncomplexed $Eu(NO_3)_3$ salt, starting from an "extracted salt" in chloroform, at 10 Å from the interface. Its behavior contrasted with the one of the $LEu(NO_3)_3$ complex (Figure 6). The salt first

attracted a "cone" of water molecules which rapidly pulled it back to the water surface (in about 40 ps). It was then captured by the aqueous phase, where it dissociated (in less than 100 ps). The Eu^{3+} cation remained at the cutoff distance from the interface, in relation with its high hydrophilicity. This behaviour is not unexpected, but raises the question of the driving force for cation migration to the interface where M^{3+} is likely captured by the ligand. It is stressed that pH and salting out effects, as well as the high concentration of uncomplexed ligands at the interface increase the cation concentration close in this region and facilitate its capture[20,34].

2.3 – *Ion recognition at the interface*

As the complexed ligand **L** is surface active, we investigated the question of ion recognition *at the interface*, in order to determine whether the binding sequence is the same in this peculiar solvent environment as in bulk methanol solution.

For this purpose, we considered a thermodynamic cycle (Scheme 2), analogous to the one presented in pure methanol, where the $\Delta G_{3\text{-wat}}$ energies for the uncomplexed M^{3+} cations were calculated in the source phase (water), while the $\Delta G_{4\text{-itf}}$ energies were calculated *at the interface*, using FEP simulations. In water, no counterions were considered, assuming that the salts are fully dissociated. At the interface, the LM^{3+} complex was surrounded by three NO_3^- counterions, considering two independent situations where either two or one anion coordinated to the cation. Computational details and results are given in Table V. The mutations were performed starting from the $LEu(NO_3)_3$ complex, after MD equilibration.

Table V shows that the $\Delta G_{4\text{-itf}}$ energies at the interface, calculated with two types of anion coordination, follow the same order as the ΔG_4 energies in methanol. They are more negative than the $\Delta G_{3\text{-wat}}$ energies. As a result, the binding selectivity, defined by $\Delta\Delta G_{itf} = \Delta G_{4\text{-itf}} - \Delta G_{3\text{-wat}}$, follows the same sequence in both environments: $Yb^{3+} > Eu^{3+} > La^{3+}$.

$$\begin{array}{ccc} Calix_{itf} + M_{1\ wat}^{3+} & \xrightarrow{\Delta G_1} & \left(Calix / M_1^{3+}\right)_{itf} \\ \Delta G_{3\text{-wat}} \downarrow & & \downarrow \Delta G_{4\text{-itf}} \\ Calix_{itf} + M_{2\ wat}^{3+} & \xrightarrow{\Delta G_2} & \left(Calix / M_2^{3+}\right)_{itf} \end{array}$$

SCHEME 2

In principle, if the conformational sampling were long enough, the simulations with one *vs* two anion coordinated to the complexed cation should converge to similar states. This was not the case, due to computer time limitations. However, the difference in $\Delta G_{4\text{-itf}}$ energies obtained in the two simulations (Table V) suggests that the binding selectivity is enhanced, when counterions are coordinated to the complexed cation.

During the mutations, the M^{3+} cation remained on the water side, at about 2 Å from the interface. Its coordination number was unchanged (CN = 9), except for the $Eu^{3+} \rightarrow Yb^{3+}$ mutation with only one coordinated NO_3^- (CN = 8: 4 O_p + 2 O_c +1 O_{NO3}+1 O_w), as one O_c coordination was lost.

3- Role of the Calixarene Platform: the $(CMPO)_4{\cdot}Eu(NO_3)_3$ complex in bulk solution and at the water / chloroform interface

3.1 – *Simulations in pure methanol or water solutions*

As **L** extracts trivalent cations much more efficiently than does CMPO itself[5], we simulated the $(CMPO)_4Eu(NO_3)_3$complex for comparison. The starting structure was obtained from the corresponding **L** complex, by removing the calix[4]arene platform and replacing the NH-phenyl by NH-Me or NH-Et groups. The uncomplexed "ligand" $(CMPO)_4$, corresponding to the four (unconnected) CMPO arms of the LEu^{3+} complex, was also considered.

A first simulation was performed in water on the $(CMPO)_4Eu(NO_3)_3$ complex, starting with

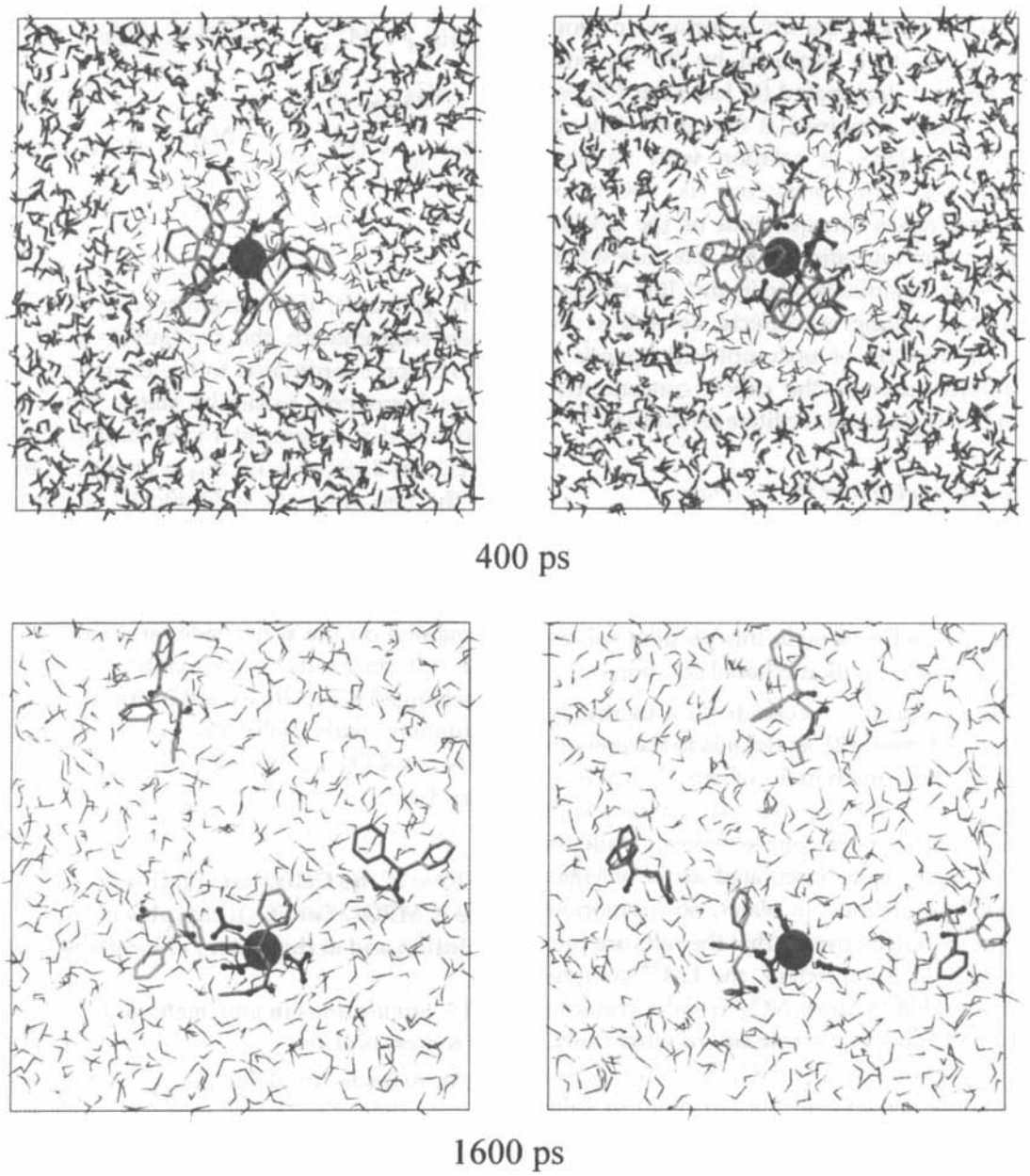

FIGURE 7 Snapshot of the $(CMPO)_4Eu(NO_3)_3$ system in water (*top*), starting with the intimate complex, and in methanol solution after 1.6 ns (*bottom*), starting with a fully dissociated complex. Orthogonal views. Drawn to different scales. The water molecules around the solute are displayed differently from those of "the bulk" for clarity (See Color Plate III at the back of this issue)

the associated arrangement, in order to test whether it would spontaneously fall apart in this solvent. This turned out not to be the case: after 400 ps of simulation, the complex rearranged to an unsymmetrical structure, where Eu^{3+} remained bound to the four O_p oxygens (2.14 ± 0.04 Å), to two O_c's (2.7 ± 0.5 Å) and to two NO_3^- monodentate anions (2.27 ± 0.02 Å), which fully

shielded the cation from water (Figure 7). Two CMPO's were monodentate, two others bidentate. The cation shielding from water prevented the dissociation of the complex. However, it is not clear whether this bound state corresponds to a thermodynamic equilibrium or to a metastable situation. The attraction energy between Eu^{3+} and the $(CMPO)_4$ "ligand" is large (780 kcal/mol) and comparable to the corresponding attraction in the **L** complex in methanol (Table III). Within the complex, each CMPO is repulsed by the three others (by about 40 kcal/mole). In the corresponding **L** complexes, this repulsion ranges from 70 to 30 kcal/mol, depending on the status of the counterions, and on the related binding mode of the CMPO arms. Thus, the comparison of the $(CMPO)_4$ *vs* **L** complexes depends on counterion effects.

A second simulation was performed on the $(CMPO)_4$, $Eu(NO_3)_3$ system in methanol solution, starting from fully dissociated CMPO's, placed at about 8 Å from the $Eu(NO_3)_3$ salt. We wanted to test whether spontaneous complexation would occur in this less dissociating solvent. After 1.6 ns (see Figure 7), the three anions remained bound to Eu^{3+}, while one CMPO moved into the first coordination shell of Eu^{3+}, whose CN was close to 9 (3 O_{NO3} + 5 O_{MeOH} + 1 $O_p$oxygen). These two simulations suggest that there likely is a significant barrier that prevents dissociation (and formation) of the 4:1 complex between 4 CMPO's and the $Eu(NO_3)_3$ salt.

3.2 – Simulations at the interface

In another set of simulations, we focused on the interfacial properties of the $(CMPO)_4Eu(NO_3)_3$ complex and of the free $(CMPO)_4$ "ligand", following their evolution, when they are initally placed at the interface.

The $(CMPO)_4Eu(NO_3)_3$ complex, initially equally shared between the two solvents, moved rapidly to the water side of the interface, where it remained until the end of the simulation (1 ns; see Figure 8). Thus, as expected, removal of the calixarene platform makes the complex more hydrophilic but the latter remains surface active. Its Eu^{3+} cation sits at about 5 Å from the interface, i.e. about 3 Å deeper in water than within the **L** complex. Its structure is similar to the one described above in pure methanol.

The uncomplexed $(CMPO)_4$ "ligand" simulated, starting from a preorganized compact arrangement, remained adsorbed at the interface until the end of the simulation (0.8 ns). However, the four CMPO's spread, and oscillated between the organic side and the aqueous side of the interface, forming (O_p···H-OH hydrogen bonds (Figure 8). Such a situation is clearly less favorable for ion capture. When the CMPO arms are anchored to a calixarene platform, they are held in close proximity at the interface, which favors the ion capture and transport compared to a dilute layer of unconnected CMPO's. It is thus stressed that, in addition to an enhanced lipophilicity, *"preorganization" of the binding sites at the interface* is an important feature for efficient ion extraction by calixarene-CMPO or related cavitand-CMPO[35, 36] ligands.

4- Discussion and conclusions

We present a modelling study of the complexes of trivalent lanthanides with a CMPO-calixarene derivative, which belongs to a new class of efficient extractant molecules for lanthanides and actinides. Based on molecular dynamics simulations, we have investigated the structures of hypothetical complexes, and calculated the binding selectivities in methanol and at a water – chloroform interface, where the cation capture and recognition presumably occurs[33].

4.1 – Stoichiometry of the complexes and coordination mode of the cation

A key question concerns the stoichiometry of the LM^{3+} complexes, which was assumed to be 1:1 throughout this study, and the number of CMPO arms involved in the cation coordination. Experimental structures of cation complexes of CMPO

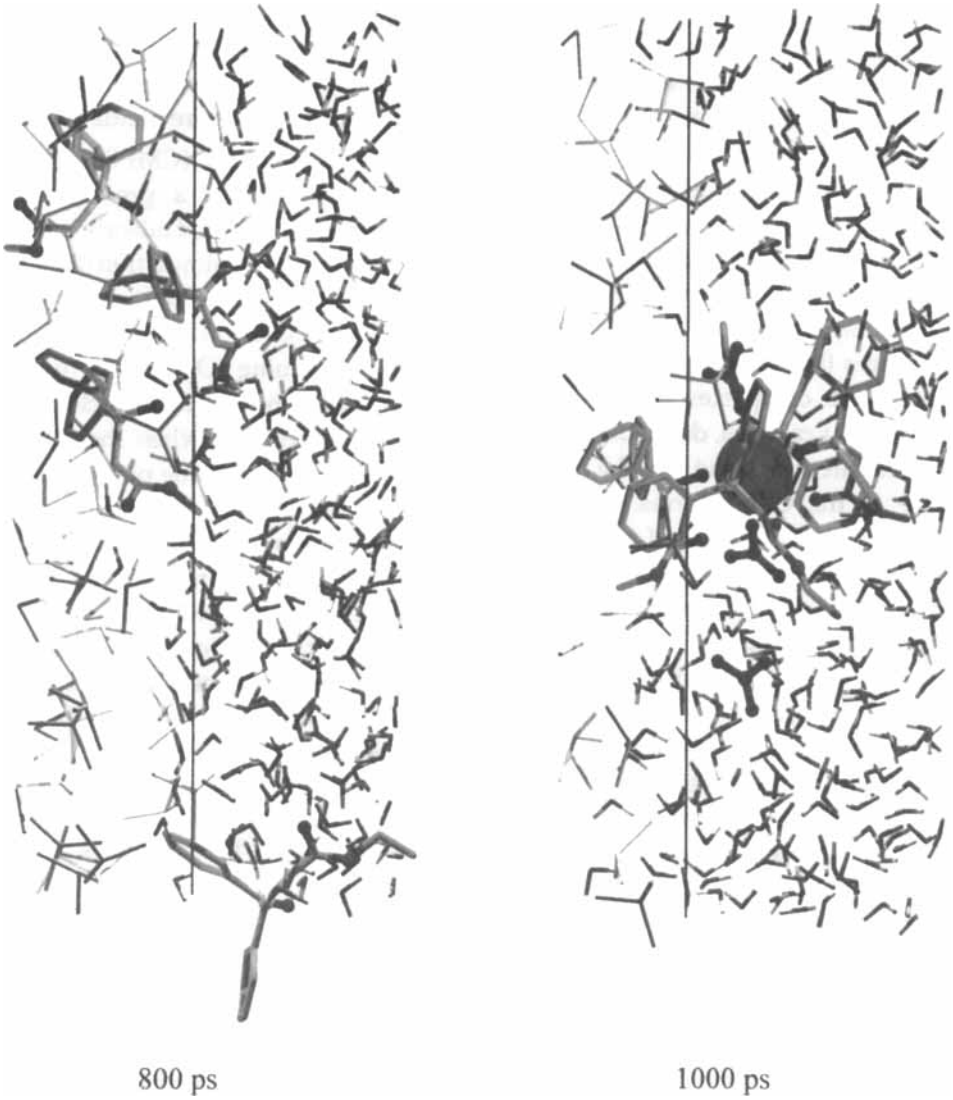

FIGURE 8 The $(CMPO)_4$ "ligand" (left; after 0.8 ns) and the $(CMPO)_4Eu(NO_3)_3$ complex (*right*; after 1 ns) systems at the interface, with selected solvent molecules. The simulations started with these solutes at the interface, with a compact arrangement extracted from the LEu^{3+} complex (see Figure 7) (See Color Plate IV at the back of this issue)

derivatives do not reveal, so far, examples of 1:4 stoichiometry. In solid state structures, the latter are generally 1:2, i.e. two CMPO's bound to M^{3+}[37,38]. Only one example of a 1:3 complex has been reported (for $Ce(NO_3)_3(CMPO)_3$[39]). In solution, CMPO complexes are generally considered to be of 1:3 type[40–43]. However, small angle neutron scattering studies have shown that CMPO and extracted praseodynium metal form large elongated polymers of 17-40 Å in diameter and up to 500 Å long, the size of which decreases if an excess of ligand is added[44]. On the computational side, a systematic study of 1:n complexes of $Eu(NO_3)_3(CMPO)_n$ has shown that

the maximum number of ligands bound to Eu^{3+} depends on the binding mode of the NO_3^- counterions[45]. The complexes have been found to be 1:2 when the three nitrates are coordinated in a bidentate mode, and 1:3 when the nitrates are monodentate. In the 1:1 complexes, the CMPO's are coordinated via both O_p and O_c oxygens while with higher stoichiometies some CMPO's are monodentate (via their O_p oxygen). In the present study we find that 1:4 CMPO complexes remain associated in water, with two NO_3^- anions coordinated to Eu^{3+}. The stoichiometry of the complex and binding mode of the CMPO's thus result from the competitive coordination of counterions and solvent molecules to the cation. Based on our studies on the **L** and $(CMPO)_4$ complexes, simultaneous binding of four CMPO's to the cation cannot be ruled out. Lower coordination by the CMPO's should correspond to the formal complexation of $M(NO_3)_n^{3-n+}$ salts.

Concerning presently available experimental data on M^{3+} complexes of **L**, no clear consistent picture emerges. The slope analysis of the distribution coefficient in liquid-liquid extraction of Eu^{3+} by **L** suggests that the complexes are of EuL_2^{3+} type[5]. We notice however that the latter have been determined with an excess of ligand and with a highly acidic aqueous phase containing an excess of NO_3^- counterions. According to recent NMR investigations in dry acetonitrile, the $Gd(ClO_4)_3$ complex of **L** forms polymeric species, even at 1:1 ligand/metal concentration ratio[46]. The NMR spectrum of $LYb(ClO_4)_3$ is consistent with dominant 1:1 complexes of C_2 symmetry. However, addition of trace amounts of water or of more complexing anions like Cl^- or NO_3^- drastically alters the spectrum, suggesting that numerous species coexist in solution and are in fast exchange on the NMR time scale[46]. According to a recent X-ray structure of $L_2Eu_5(NO_3)_{15}.2H_20$, one $Eu(NO_3)_3$ moiety is coordinated to CMPO arms belonging to different calixarene units[47]. In other complexes **L** binds two La^{3+} or Eu^{3+} cations, each of them belonging to a $M(NO_3)_2$ moiety coordinated to two arms only[47]. Thus, *the stoichiometry of the complexes and the binding mode of the cation seem to be highly versatile and environment dependent.* Our analysis strongly suggests that, in addition to cation-ligand interactions, counterions play a major role. They have to be either well solvated, or directly coordinated to the cation.

After our calculations were completed, two series of experimental data concerning the complexation of M^{3+} cations by **L** became available.[6] The first one concerns the extraction of lanthanides and actinides from highly saline or acidic media by **L**, where the order of cation selectivities was $La^{3+} > Eu^{3+} > Yb^{3+}$, inversed to the one we calculated at the interface[6]. It is not clear whether this difference is due to computational artefacts (see below), or to the different nature of the extracted species which remains to be investigated as a function of the concentrations of salts, ligands, and cations. Interestingly, when the phenyl $OPPh_2$ substituents of **L** were replaced by alkyl $OP(C_6H_{13})_2$ ones, the extraction selectivity disappeared[6]. This is contrary to expectations from polarization effects, which should enhance the preference for the hardest cation Yb^{3+} in the case of phenyl, compared to alkyl substituents[48]. The second series of experiments concerns the complexation of lanthanide cations by **L** in methanol solution, where no clear selectivity was found and a mixture of 1:1, 2:1 and 1:2 species are likely present[49]. When compared to our calculations, these data suggest that calculations overestimate the interactions of **L** with Yb^{3+}, relative to La^{3+}. In the following, we discuss the electrostatic representation of the system, as a possible source for discreprancy.

4.2 – Computational aspects. Polarization and Charge transfer effects

Non-covalent interactions involving trivalent lanthanide cations are difficult to model by force fields, due to the hardness of the cation and related polarization and charge transfer effects. According to QM calculations[48,50] the latter are not constant but are cation dependent. The

cationic charge also depends on the environment and coordination of counterions. For instance, the Mulliken charge of Eu^{3+} drops from 2.46 e in the $Eu\cdots OPPh_3{}^{3+}$ complex (no counterion) to 1.37 e in the $Cl_3Eu\cdots OPPh_3$ complex[48]. It remains thus to be assessed whether a simple force field representation of trivalent lanthanide cations represented with a 3+ charge and using pairwise additive 1–6–12 potentials, without an explicit polarization term, yields correct structural and energetical features of the complexes. According to the QM calculations, phenyl substituents on the phosphoryl group enhance their interactions with lanthanide cations, compared to alkyl ones[48]. This feature, consistent with experimental data obtained for derivatives of **L**[5] can hardly be accounted for by simple force field 1–6–12 potentials.

The prediction of binding selectivities represents a computational challenge as it requires an accurate representation of the potential energy of the system, and an adequate sampling of its conformational states. Concerning the sampling problem, we investigated a number of structures different from those described above, involving less than four arms wrapping around the cation and some counterions directly coordinated to the M^{3+} cation. After 1 ns of simulation, they all yielded different structures, differing from the ones described here. This thus shows that the conformational sampling of complexes with highly charged cations remains problematic[51,52]. In addition, as emphasized above, the nature of the complexes and precise binding mode of the cation depend on concentration and medium effects (counterions, pH and solvent).

In relation with the energy representation of the complexes, we tested alternative electrostatic representations, which might reduce the ΔG_4 energies (Scheme 1), and possibly less favour the complexation of Yb^{3+} compared to Eu^{3+} and La^{3+}. Due to computer limitations, we estimated the binding selectivity as $\Delta\Delta G = \Delta G_{4\text{-gas}} - \Delta G_{3\text{-wat}}$, where $\Delta G_{4\text{-gas}}$ is calculated in the gas phase. Six electrostatic models *A* to *F* were tested. The results are described in Table VI. Compared to the standard model *A*, the models *B* and *C* correspond to a cationic charge reduction from 3.0 to 2.5 and 2.0 e, keeping the ligand **L** unchanged. The model *A* yields $\Delta G_{4\text{-gas}}$ energies close to the $\Delta G_{4\text{-wat}}$ ones, and leads therefore to the same binding sequence ($Yb^{3+} > Eu^{3+} > La^{3+}$) as calculated in pure solution, while models *B* and *C* lead to inversed sequences of binding (Table VI). The models *D* and *E* correspond to reduced charges (divided by 1.2), either on all atoms of the LM^{3+} solute (*E*) or on the **L** atoms only (*D*). They lead to still other orders of selectivities (Table VI). These tests thus indicate that a smaller difference in Yb^{3+} / La^{3+} binding affinities is obtained either with a reduced charge on the cation (2.5 e; model *B*) or when a uniform scaling factor is applied on all solute charges (model *E*). Such procedures are however not satisfactory, the first reason being that they do not conserve the total +3 charge on the LM^{3+} complex. Second, in models *E* or *D*, the charge of the phosphoryl oxygen (-0.766 e) is less negative than the O_{H_2O} charge (-0.834 e), which is not consistent with the fact that the phosphoryl group interacts better than does a water molecule with a given cation[50]. Alternative procedures have been presented to mimic charge transfer from the cation to the ligands in its first coordination sphere[10], but they are presently restricted to static cation coordination[53], without possibility of ligand exchange.

Another issue concerns polarization effects which are generally considered to improve the electrostatic representation of the system[32,54]. We therefore tested a polarized model of LM^{3+} where **L** is described as in the standard calculations above, plus an additional polarization term (see ref.[55]) using the atomic polarizabilities of ref.[56]. The results (Table VI; model *F*) show that this model increases the preference for Yb^{3+} over La^{3+}, compared to the standard 1–6–12 representation of non-bonded interactions, and therefore exaggerates the preference for Yb^{3+} complexation.

TABLE VI Energy results (kcal/mol) from FEP simulations on the LM^{3+} complexes *in vacuo*. [a] Comparison of six electrostatic models

Model	*FEP conditions*	ΔG_4 (LM^{3+}) *(in vacuo)*		$\Delta\Delta G$ (LM^{3+}) [b]		*Selectivity order*
		$La^{3+} \rightarrow Eu^{3+}$	$Eu^{3+} \rightarrow Yb^{3+}$	$Eu^{3+} \rightarrow La^{3+c}$	$Yb^{3+} \rightarrow La^{3+c}$	
A	ε_r=1, q_M = 3.0	−69.9	−58.7	−18.5	−27.2	Yb>Eu>La
		(−69.7) [d]	(−56.8) [d]			
B	ε_r=1, q_M = 25	−52.5	−44.3	−1.1	+44.6	Eu>La>Yb
C	ε_r=1, q_M = 2.0	−36.4	−34.4	+15.0	+30.6	La>Eu>Yb
D	ε_r=1.2, q_M =3.6	−74.4	−62.7	−23.0	−35.7	Yb>Eu>La
E	ε_r=1.2, q_M = 3.0	−56.8	−48.1	−5.4	−3.5	Eu>Yb>La
F	ε_r=1, q_M= 3.0, polarizability[e]	−86.5	−78.2	−35.1	−63.3	Yb>Eu>La

a. Mutation performed in 51 windows (2 + 3 ps) with a 100Å cutoff.
b. $\Delta\Delta G = \Delta G_{4\text{-vacuo}} - \Delta G_{3\text{-exp}}$.
c. Free energy of complexation relative to the La^{3+} complex.
d. ΔG_4 in pure water (no counterions).
e. Polarizabilities are adapted from ref.[56] (α_C = 0.878, $\alpha_{C\ carbonyl}$ = 0.616, α_H = 0.135, $\alpha_{O\ ether}$ = 0.465, $\alpha_{O\ CO/PO}$ = 0.434, α_N = 0.530) or estimated (α_P = 1.5).

Taken together these results suggest that improved force field representations should simultaneously account for the charge transfer from the cation to the ligand, and for the polarization of the latter. Alternative promising approaches (QM/MM) combine a quantum mechanical representation of the solute and a force field representation of the surrounding system[57–59].

4.3 – *Importance of interfacial phenomena in liquid-liquid cation extraction*

Although no experimental results that could elucidate the mechanism of cation extraction by CMPO-calixarenes are available, it can be stressed that *ion complexation and recognition take place at water – organic liquid boundary*[60–63]. This is supported by the fact that the uncomplexed ligands display amphiphilic character and are surface active. They should thus be more concentrated at the interface than in the bulk organic phase. We notice that in the extraction experiments that have been reported, the aqueous phase is acidified[5,6,64]. This presumably leads to enhanced hydrogen bonding between the phosphoryl oxygens of the CMPO's and the $H_5O_2^+$ species[65], or to protonation of these phosphoryl groups at the interface which enhances their surface activity, as observed for TBP[66,67]. The nature of CMPO-calixarene assemblies at the interface is not known, as it may range from more or less ordered saturated monolayers to disordered aggregates. The cone shape of the derivatives of **L** bearing O-alkyl chains at the lower rim does not seem to be best suited to form a regular monolayer at a flat interface. It is better suited for curved surfaces, like those of micelles or of microdroplets formed when the extraction system is mixed. As far as the cation complexes of the extractant molecules are concerned, they are more amphiphilic than the free extractants and should be more concentrated at the interface. Given their reluctance to move to the water side of the interface, it can be speculated that *ion capture and recognition take place at the liquid-liquid interface.* This is supported

by experiments at the water-air interface[68–70] and by computations[33] on related systems. This mechanism requires however that the uncomplexed cation can approach the interfacial ligands, which seems in contradiction with our results on the $Eu(NO_3)_3$ salt or on related salts[34], which are "repelled" by the interface and dissociated in water. We suggest that the high concentration of NO_3^- anions in the aqueous phase increases the concentration of the $Eu(NO_3)_n^{3-n+}$species (n>1), which are less hydrophilic and more surface active than the dissociated Eu^{3+} cation. This argument is also in favor of the complexation of $Eu(NO_3)_n^{(3-n)+}$ species, leading to reduced interactions between CMPO ligands and the cation, and to stoichiometries larger than 1:1. Related simulations are in progress at MSM[71].

To conclude, it appears that modelling lanthanide cation complexes of calix[4]arene-CMPO type ligands remains a difficult task, as long as the nature of the species involved is not established from experiment. It raises a number of stimulating computational problems, which cannot easily be solved, even when reasonable cation parameters are available. At present, the questions of stoichiometry, counterion effects and binding mode of lanthanide complexes can hardly be solved by computations only, as the corresponding relaxation times are much longer than those of monovalent cation complexes. Our study should foster further experimental investigations of the nature, structure and thermodynamic properties of lanthanide complexes in homogeneous liquid phases, as well as at liquid-liquid interfaces.

Acknowledgements

The authors are grateful to CNRS-IDRIS and to Université Louis Pasteur for allocation of computer resources. The authors thank the EEC (F14W-CT96–0022 contract) for support. MB thanks the french ministery of research for a grant.

References

[1] Cecille, L.; Casarci, M.; Pietrelli, L. *New Separation Chemistry Techniques for Radioctive Waste and other Specific Applications.*; **1991**, Commission of the European Communities; Elsevier Applied Science: London New York.
[2] Rozen, A. M., (1990) *J. Radioanal. Nucl. Chem., Articles*, **143**, 337–355.
[3] Nash, K. L., (1993) *Solv. Extract. Ion Exch.*, **11**, 729–768.
[4] Schwing-Weil, M.-J.; Arnaud-Neu, F., (1997) *Gazz. Chim. Ital.*, **127**, 687–692.
[5] Arnaud-Neu, F.; Böhmer, V.; Dozol, J.-F.; Grüttner, C.; Jakobi, R. A.; Kraft, D.; Mauprivez, O.; Rouquette, H.; Schwing-Weil, M.-J.; Simon, N.; Vogt, W., (1996) *J. Chem. Soc. Perk. 2*, 1175–1182.
[6] Delmau, L. H.; Simon, N.; Schwing-Weill, M.-J.; Arnaud-Neu, F.; Dozol, J.-F.; Eymard, S.; Tournois, B.; Böhmer, V.; Grüttner, C.; Musigmann, C.; Tunayar, A., (1998) *J. Chem. Soc. Chem. Comm.*, 1627–1628.
[7] Delmau, P., *Extraction de lanthanides et d'actinides trivalents par des calixarènes fonctionnalisés. Etude structurale des complexes en solution par RMN*, **1997**, Thesis, Université Louis Pasteur, Strasbourg.
[8] Katz, J. J.; Seaborg, G. T.; Morss, L. R. *The Chemistry of the Actinide Elements, 2nd Ed.*; Chapman and Hall; London, 1986.
[9] Seaborg, G. T., (1993) *Radiochimica Acta*, **61**, 115–122.
[10] Beech, J.; Drew, M. G. B.; Leeson, P. B., (1996) *Structural Chemistry*, **7**, 153–165.
[11] van Veggel, F. C. J. M.; Reinhoudt, D., (1999) *Chem. Eur. J.*, **5**, 90–95. G. W. thanks the authors for providing the parameters prior publication.
[12] Åqvist, J., (1990) *J. Phys. Chem.*, **94**, 8021–8024.
[13] Wipff, G.; Engler, E.; Guilbaud, P.; Lauterbach, M.; Troxler, L.; Varnek, A., (1996) *New J. Chem.*, **20**, 403–417.
[14] Varnek, A.; Wipff, G., (1996) *J. Comput. Chem.*, **17**, 1520–1531.
[15] Lauterbach, M.; Wipff, G. in *Physical Supramolecular Chemistry*, L. Echegoyen, A. Kaifer Ed., Kluwer Acad. Pub., Dordrecht, 1996, pp 65–102.
[16] Guilbaud, P.; Wipff, G., (1996) *New J. Chem.*, **20**, 631–642.
[17] Varnek, A.; Troxler, L.; Wipff, G., (1997) *Chem. Eur. J.*, **3**, 552–560.
[18] Lauterbach, M.; Mark, A.; van Gunsteren, W.; Wipff, G., (1997) *Gazzetta Chim. Ital.*, **127**, 699–709.
[19] Beudaert, P.; Lamare, V.; Dozol, J.-F.; Troxler, L.; Wipff, G., (1998) *Solv. Extract. Ion Exch.*, **16**, 597–618.
[20] Berny, F.; Muzet, N.; Schurhammer, R.; Troxler, L.; Wipff, G. in *Current Challenges in Supramolecular Assemblies, NATO ARW Athens*, G. Tsoucaris Ed., Kluwer Acad. Pub., Dordrecht, 1998, pp 221–248.
[21] Pearlman, D. A.; Case, D. A.; Caldwell, J. C.; Ross, W. S.; Cheatham III, T. E.; Ferguson, D. M.; Seibel, G. L.; Singh, U. C.; Weiner, P.; Kollman, P. A., (1995) *AMBER4. 1*,.
[22] Cornell, W. D.; Cieplak, P.; Bayly, C. I.; Gould, I. R.; Merz, K. M.; Ferguson, D. M.; Spellmeyer, D. C.; Fox, T.; Caldwell, J. W.; Kollman, P. A., (1995) *J. Am. Chem. Soc.*, **117**, 5179–5197.
[23] Wipff, G.; Lauterbach, M., (1995) *Supramol. Chem.*, **6**, 187–207.
[24] Jorgensen, W. L.; Chandrasekhar, J.; Madura, J.D., (1983) *J. D.*, (1983) *J. Chem. Phys.*, **79**, 926–936.

[25] Jorgensen, W. L.; Briggs, J. M.; Contreras, M. L., (1990) *J. Phys. Chem.*, **94**, 1683–1686.

[26] Lauterbach, M.; Engler, E.; Muzet, N.; Troxler, L.; Wipff, G., (1998) *J. Phys. Chem.*, **102**, 225–256.

[27] Engler, E.; Wipff, G. in *"Crystallography of Supramolecular Compounds"*, G. Tsoucaris Ed., Kluwer, Dordrecht, 1996, pp 471–476.

[28] Kollman, P., (1993) *Chem. Rev.*, **93**, 2395–2417.

[29] Jorgensen, W. L., (1989) *Acc. Chem. Res.*, **22**, 184–189.

[30] Marcus, Y. *Ion Solvation.*; Wiley: Chichester, 1985.

[31] Bünzli, J.-C.; Milicic-Tang, A. in *Handbook on the Physics and Chemistry of Rare Earths.*, K. A. Gschneidner Jr, L. Eyring Ed., Elsevier Science B.V., 1995, pp 306–359.

[32] Kowall, T.; Foglia, F.; Helm, L.; Merbach, A. E., (1995) *J. Am. Chem. Soc.*, **117**, 3790–3799.

[33] Muzet, N.; Engler, E.; Wipff, G., (1998) *J. Phys. Chem. B*, **102**, 10772–10788.

[34] Berny, F.; Muzet, N.; Troxler, L.; Wipff, G. in *Supramolecular Science: where it is and where it is going*, R. Ungaro, E. Dalcanale Ed., Kluwer Acad. Pub., Dordrecht, 1999, pp 95–125.

[35] Boerrigter, H.; Verboom, W.; Reinhoudt, D. N., (1997) *Liebigs Ann./Recueil*, 2247–2254.

[36] Boerrigter, H.; Verboom, W.; Reinhoudt, D. N., (1997) *J. Org. Chem.*, **62**, 7148–7155.

[37] Stewart, W. E.; Siddall, T. H., (1970) *J. Inorg. Nucl. Chem.*, **32**, 3599.

[38] Bowen, S. M.; Duesler, N.; Paine, R. T., (1982) *Inorg. Chim. Acta*, **61**, 155–166.

[39] Babecki, R.; Platt, A. W. G.; Russel, D. R., (1990) *Inorg. Chim. Acta*, 25–28.

[40] Du Preez, R.; Preston, J. S., (1986) *S-Afr. J. Chem.*, **39**, 137–142.

[41] Bednarczyk, L.; Siekierski, S., (1989) *Solv. Extract. Ion Exch.*, 7, 273–287.

[42] Nakamura, T.; Miyake, C., (1994) *Solv. Extract. Ion Exch.*, **12**, 931.

[43] Reddy, M. L. P.; Damodaran, A. D.; Mathur, J. N.; Murali, M. S.; Balarama Krishna, M. V.; Iyer, R. H., (1996) *Solv. Extract. Ion Exch.*, **14**, 793–816. Diamond, H.; Horwitz, E. P.; Danesi, P. R., (1986) *Solv. Extract. Ion Exch.*, **4**, 1009.

[44] Diamond, H. ; Thiyagarajan, P. ; Horwitz, E. P., (1990) *Solvent Extr. & Ion Exch.*, **8**, 503-513. Aggregates of metal complexes of phosphonic acid derivatives have also been characterized by SANS. See chiariza, R. ; Urban, V. ; Thiyagarajan, P. ; Herlinger, A. W., (1999) *Solv. Extract. Ion Exch.*, **17**, 113-132.

[45] Beudaert, P.; Lamare, V.; Dozol, J.-F. ; Troxler, L. ; Wipff, G., (1999) *J. Chem. Soc. Perkin Trans*, 2515-2524.

[46] Lambert, B. ; Jacques, V. ; Shivanyuk, A. ; Matthews, S. E. ; Tunayar, A. ; Baaden, M. ; Wipff, G. ; Böhmer, V. ; Desreux, J.-F., (2000) *Inorg. Chem.*, **39**, 2033–2041.

[47] Böhmer, V. ; Nierlich, M., (private communcation). Cherfa, S., (1998) *Etude structurale de la complexation de l'uranyle et des ions lanthanides par des calixarenes fonctionnalisés par le CMPO* ; Thesis, Université de Paris-Sud Orsay.

[48] Troxler, L.; Dedieu, A. ; Hutschka, F.; Wipff, G., (1998) *J. Mol. Struct (THEOCHEM)*, **431**, 151–163.

[49] Arnaud-Neu, F.; Schwing, M.-J.; Böhmer, V., (private communcation). Arnaud, F. in *Calixarènes for Separation. ACS Symposium series 757*, G. Lumetta, R. Rogers, A. Gopolan Ed., ACS, Washington DC, 2000, in press.

[50] Berny, F.; Muzet, N.; Troxler, L.; Dedieu, A.; Wipff, G., (1999) *Inorg. Chem.*, **38**, 1244-1252. Baaden, M. ; Berny, F. ; Boehme, C. ; Muzet, N. ; Schurhammer, R. ; Wipff, G., (2000) *J. Alloys Compounds*, **303–304**, 104–111. Schurhammer, R. ; Erhart, V. ; Troxler, L. ; Wipff, G., (1999) *J. Chem. Soc. Perkin Trans.*, 2515-2534.

[51] Fraternali, F.; Wipff, G., (1997) *J. Phys. Org. Chem.*, **10**, 292–304.

[52] van Veggel, F. C. J. M., (1997) *J. Phys. Chem. A*, **101**, 2755–2765.

[53] Hay, B., (1993) *Coord. Chem. Rev.*, **126**, 177–236 and references cited therein.

[54] Kollman, P. A., (1996) *Acc. Chem. Res.*, **29**, 461–469.

[55] Sun, Y.; Caldwell, J. W.; Kollman, P. A., (1995) *J. Phys. Chem.*, **99**, 10081–10085.

[56] Applequist, J.; Carl, J. R.; Fung, K.-K., (1972) *J. Am. Chem. Soc.*, **94**, 2952–2960.

[57] Thompson, M. A.; Glendening, E. D.; Feller, D., (1994) *J. Am. Chem. Soc.*, **116**, 10465–10476.

[58] Stanton, R. V.; Little, L. R.; Merz, K. M., (1995) *J. Phys. Chem.*, **99**, 483–486.

[59] Gao, J., (1996) *Acc. Chem. Res.*, **29**, 298–305.

[60] Watarai, H., (1993) *Trends in Analytical Chemistry*, **12**, 313–318.

[61] Moyer, B. A. in *Molecular Recognition: Receptors for Cationic Guests*, J. L. Atwood, J. E. D. Davies, D. D. McNicol, F. Vögtle, J.-M. Lehn Ed., Pergamon, 1996, pp 325–365 and references cited therein.

[62] Vandegrift, G. F.; Horwitz, E. P., (1980) *J. Inorg. Nucl. Chem.*, **42**, 119–125.

[63] Danesi, P. R. in *Principles and Practices of Solvent Extraction*, J. Rydberg, C. Musikas, G.R. Chopin Ed., M. Dekker, Inc., New York, 1992, pp 157–207.

[64] Malone, J. F.; Marrs, D. J.; McKervey, A.; O'Hagan, P.; Thompson, N.; Walker, A.; Arnaud-Neu, F.; Mauprivez, O.; Schwing, M.-J.; Dozol, J.-F.; Rouquette, H.; Simon, N., (1995) *J. Chem. Soc. Chem. Commun.*, 2151–2153.

[65] Stoyanov, E., (1998) *J. Chem. Soc. Farad. Trans*, **94**, 2803–2812.

[66] Tomoaia, M.; Andrei, Z.; Chifu, E., (1973) *Rev. Roum. Chim.*, **18**, 1547.

[67] Chifu, E.; Andrei, Z.; Tomoaia, M., (1974) *Anal. Chim. (Rome)*, **64**, 869–871.

[68] Ishikawa, Y.; Kunitake, T.; Matsuda, T.; Otsuka, T.; Shinkai, S., (1989) *J. Chem. Soc. Chem. Commun.*, 736–737.

[69] Dei, L.; Casnati, A.; Nostro, P. L.; Baglioni, P., (1995) *Langmuir*, **11**, 1268–1272.

[70] Nostro, P. L.; Casnati, A.; Bossoletti, L.; Dei, L.; Baglioni, P., (1996) *Colloids and Surfaces A*, **116**, 203–209.

[71] Baaden, M. ; Berny, F. ; Muzet, N. ; Troxler, L. ; Wipff, G. in *Calixarenes for Separation. ACS Symposium series 757*, G. Lumetta, R. Rogers, A. Gopolan Ed., ACS, Washington DC, 2000, pp 71-85. Baaden, M. ; Berny, F. ; Wipff, G., (2000) *J. Mol. Liquids*, in press.